2013

HYSTERESIS IN REPOLARIZATION OF CARDIAC ACTION POTENTIALS: EFFECTS OF SPATIAL HETEROGENEITY AND SLOW REPOLARIZATION CURRENTS

Linyuan Jing
University of Kentucky, jinglinyuan2008@gmail.com

STUDENT AGREEMENT:

I represent that my thesis or dissertation and abstract are my original work. Proper attribution has been given to all outside sources. I understand that I am solely responsible for obtaining any needed copyright permissions. I have obtained and attached hereto needed written permission statements(s) from the owner(s) of each third-party copyrighted matter to be included in my work, allowing electronic distribution (if such use is not permitted by the fair use doctrine).

I hereby grant to The University of Kentucky and its agents the non-exclusive license to archive and make accessible my work in whole or in part in all forms of media, now or hereafter known. I agree that the document mentioned above may be made available immediately for worldwide access unless a preapproved embargo applies.

I retain all other ownership rights to the copyright of my work. I also retain the right to use in future works (such as articles or books) all or part of my work. I understand that I am free to register the copyright to my work.

REVIEW, APPROVAL AND ACCEPTANCE

The document mentioned above has been reviewed and accepted by the student's advisor, on behalf of the advisory committee, and by the Director of Graduate Studies (DGS), on behalf of the program; we verify that this is the final, approved version of the student's dissertation including all changes required by the advisory committee. The undersigned agree to abide by the statements above.

Linyuan Jing, Student

Dr. Abhijit Patwardhan, Major Professor

Dr. Abhijit Patwardhan, Director of Graduate Studies

HYSTERESIS IN REPOLARIZATION OF CARDIAC ACTION POTENTIALS: EFFECTS OF SPATIAL HETEROGENEITY AND SLOW REPOLARIZATION CURRENTS

DISSERTATION

A dissertation submitted in partial fulfillment of
the requirements for the degree of Doctor of Philosophy in the
College of Engineering at the University of Kentucky

By

Linyuan Jing

Lexington, Kentucky

Director: Dr. Abhijit Patwardhan, Professor of Biomedical Engineering

Lexington, Kentucky

2013

ABSTRACT OF DISSERTATION

HYSTERESIS IN REPOLARIZATION OF CARDIAC ACTION POTENTIALS: EFFECTS OF SPATIAL HETEROGENEITY AND SLOW REPOLARIZATION CURRENTS

Repolarization alternans, i.e. beat-to-beat variation of repolarization of action potential, is proposed as a predictor of life-threatening arrhythmias. Restitution relates repolarization duration with its previous relaxation time, i.e. diatstolic interval (DI), and is considered a dominant mechanism for alternans. Previously, we observed that different repolarization durations at the same DI during decelerating and accelerating pacing, i.e. restitution displays hysteresis, which is a measure of "cardiac memory".

Objective of the current study was to investigate in the pig 1) the mechanism for a previously observed hysteresis type phenomenon, where alternans, once started at higher heart rate, persists even when heart rate decreases below its initiating rate, 2) regional differences in expression of hysteresis, i.e. memory in restitution in the heart, and 3) changes in restitution and memory during manipulation of an important repolarization current, the slow delayed rectifier, I_{Ks}.

Action potentials were recorded in pig ventricular tissues using microelectrodes. Regional differences were explored in endocardial and epicardial tissues from both ventricles. DIs were explicitly controlled in real time to separate restitution mechanism from non-restitution related effects. Stepwise protocols were used to explore the existence in hysteresis in alternans threshold, where DIs were held constant for each step and progressively decreased and then increased. Quantification of cardiac memory was achieved by sinusoidally changing DI protocols, which were used to investigate memory changes among myocytes from different regions of the heart and during I_{Ks} manipulation.

Results show that during stepwise protocol, hysteresis in alternans still existed, which indicates that restitution is not the only mechanism underlying the hysteresis. When comparing hysteresis obtained from sinusoidally oscillatory DIs among different regions, results show memory is expressed differently with endocardium expressing the most and epicardium the least memory. This provides important implications about the location where arrhythmia would initiate. Results also show that measures for hysteresis loops

obtained by sinusoidal DI protocols decreased (increased) after enhancement (attenuation) of I_{Ks}, suggesting decreased (increased) hysteresis, i.e. memory in restitution. This effect needs to be considered during drug development.

KEYWORDS: Arrhythmia, Restitution, Repolarization Alternans, Action Potential Duration, Cardiac Memory.

Linyuan Jing

July 18, 2013

HYSTERESIS IN REPOLARIZATION OF CARDIAC ACTION POTENTIALS: EFFECTS OF SPATIAL HETEROGENEITY AND SLOW REPOLARIZATION CURRENTS

By

Linyuan Jing

Abhijit Patwardhan, Ph.D.

Director of Dissertation

Abhijit Patwardhan, Ph.D.

Director of Graduate Studies

July 18, 2013

DEDICATION

I dedicate this dissertation to my family, especially…

to my parents, for supporting me each step of the way;

to grandma, for early childhood education and encouragement;

to my fiancé Qingguang, for continued love and understanding

—may you also be motivated and encouraged to reach your dreams.

Acknowledgements

I would like to acknowledge my advisor, Dr. Abhijit Patwardhan for his patience, encouragement and indispensable knowledge. Completion of this dissertation would have been impossible without his continual support, invaluable ideas and guidance throughout the entire course of my graduate studies.

I would also like to acknowledge the members of my Dissertation Committee: Dr. Knapp, Dr. Randall, and Dr. Yu, and my outside examiner Dr. Gregory Frolenkov for his valuable input to my dissertation.

Table of Contents

List of Tables

List of Figures

Chapter I Introduction

Sudden cardiac death, also called sudden cardiac arrest, describes a situation when death is caused by abrupt cardiac electrical malfunction that develops in a short period of time, usually within an hour. Each year, sudden cardiac death accounts for more than 300,000 deaths in the United States for the past few decades, and is responsible for half of the mortality caused by heart disease [1]. Ventricular tachycardia (VT), when the heart rhythm becomes very fast, usually > 120 beats/minute, or ventricular fibrillation (VF), when the heart suddenly starts quivering and stops pumping blood to the body, is the most common arrhythmia that causes cardiac arrest. Sudden cardiac arrest can be reversed by CPR (cardiopulmonary resuscitation) or defibrillation, however, the treatment needs to be received within 5-7 minute after occurrence of the cardiac arrest to increase the survival rate to 30-45%, otherwise, survival rate is decreased by 7-10% for every minute before defibrillation is provided [2, 3].

Given the high mortality rate, understanding the mechanisms and predicting the occurrence of cardiac arrhythmia, especially VF, becomes very important. The dominant mechanism of VF has been proposed as reentry, i.e. reactivation of myocardial tissue that has been recently activated by the same impulse. Development of re-entrant arrhythmia at cellular level has been closely related to the stability of action potential duration (APD). It is widely known that T-wave alternans, i.e. beat-to-beat variation in the amplitude or shape of the T wave in an electrocardiogram (ECG), is associated with sudden cardiac death [4-6] and has been used as a predictor for arrhythmia [7-11]. Alternans of APD, a beat-to-beat variation in successive APDs, which is the cause of T-wave alternans in

ECG, is thought to presage and be conducive to VF. Several hypotheses have been proposed to explain the stability of electrical activation and inducibility of alternans. Prominent among these are: 1) restitution of APD [12, 13], which relates the current APD with its preceding diastolic interval (DI), and 2) electrical memory in restitution [14], which in this context, refers to the dependence of an APD on previous APDs over a period of several seconds [15, 16]. Note that cardiac memory in the field of electrophysiology is a somewhat diffuse term and although it can have a different meaning such as long term remodeling due to elevated afterload, in the context of the current study, it is used to mean the relationship between the current APD and previous APDs to be consistent with the literature. In restitution hypothesis, a steep restitution curve has been mechanistically linked to electrical instability and initiation of alternans of APD, however, in our previous study [17], we reported that alternans of APD could occur independent of changes in preceding DI, suggesting that other mechanisms besides restitution play an important role in occurrence of alternans. Additionally, recent studies showed that memory in restitution may also play an important role in stability of activation [18-20]. A detailed explanation of restitution and memory mechanisms will be provided in Chapter II. We have shown previously [15, 16, 21] that an oscillatory DI protocol where DIs were explicitly controlled in real time and changed in sinusoidal pattern, can be used to quantify memory, which is observed as hysteresis in restitution. Although the restitution mechanism and its role in arrhythmia generation have been extensively investigated by many studies, less is known about the characteristics of hysteresis, i.e. memory effect.

1.1 Objective and Specific Aims for the Dissertation

Objective for this dissertation is to explore the existence of hysteresis, i.e. memory in repolarization of action potential and investigate the effect of spatial heterogeneity and slow repolarization currents on the characteristics of hysteresis. The experiments were conducted in the pig, a widely used species to study the link between restitution and arrhythmia in previous studies [18, 22]. The specific aims for the study are as follows:

Specific Aim 1: Explore the existence of hysteresis in threshold for onset and termination of APD alternans during DI independent pacing protocols to determine whether restitution is the underlying mechanism of this hysteresis. Hysteresis in threshold for onset and termination of APD alternans, i.e. hysteresis in the transition between 1:1 (normal) rhythm and 2:1 (block) or 2:2 (alternans) rhythms, has been reported in previous studies [23-25], the transition from 2:1 or 2:2 rhythms back to 1:1 rhythm occurred at longer cycle length (CL) than the transition from 1:1 to 2:1 or 2:2 rhythm. In our previous study [17], we reported that alternans of APD could occur independent of changes in preceding DI, suggesting that other mechanisms besides restitution play an important role in occurrence of alternans. However, in those previous studies investigating hysteresis in the state transition [23-25], pacing was performed using constant CLs. Thus, changes in APDs would always be accompanied by changes in DIs, which means constant involvement of restitution. Therefore, it was impossible to determine whether hysteresis also existed in the restitution independent mechanism of alternans. An example of such restitution independent mechanism in onset threshold of alternans would be cardiac memory. To accomplish aim 1, we used a novel protocol where DIs were explicitly controlled in real time. This novel DI protocol allows us to

investigate the existence of hysteresis in alternans threshold when restitution dependent mechanism is excluded. In the following chapters of the dissertation, this phase of the study is referred as phase 1 of the study, or study of hysteresis in alternans threshold.

Specific Aim 2: Investigate the existence of spatial heterogeneity in hysteresis, i.e. memory, in endocardial and epicardial tissues of both left and right ventricles in the pig hearts. Heterogeneity in dynamics of action potential repolarization has been reported to increase dispersion of repolarization and thus, promote discordant alternans which could then lead to block and reentrant circuit [20, 26-30]. It has been shown that restitution is different among different regions of the heart and that instability also may be initiated heterogeneously [20, 22, 26-33]. Although restitution, and heterogeneity in it, has been investigated extensively using Guinea pig and rabbit models and in a few studies in the pig, quantification of memory, and heterogeneity in its expression, is not widely known. While there have been a few studies where indirect measures of memory were obtained on the epicardial surface of a rabbit epicardium [32, 34], differences in memory between the endocardium and the epicardium, especially in a larger animal model such as the pig are not known. Considering the critical role of spatial heterogeneity in conduction of an action potential, it becomes important to investigate whether memory is different among different regions of the heart. Hysteresis in restitution was obtained using a novel DI protocol where DI oscillates sinusoidally. This protocol has been shown in our previous studies [15, 16, 21] as a good method to quantify memory. This phase of the study will be referred as phase 2 of the study, or heterogeneity study in the following chapters.

<u>Specific Aim 3</u>: Determine the effect of changes in an important repolarization current, slow delayed rectifier potassium current (I_{Ks}), on memory and restitution in action potential repolarization. I_{Ks} plays a critical role in late repolarization phase of an action potential by serving as a repolarization reserve when other repolarization currents, e.g. rapid delayed rectifier potassium current (I_{Kr}), are reduced during diseased conditions or during drug interaction. Although prolongation of APD is proposed to be proarrhythmic in situations such as long QT syndrome, there is also evidence showing that lengthening of APD at short CL, i.e. higher heart rate, is an effective way to suppress re-entrant arrhythmia as it reduces dispersion of repolarization in different areas of the heart. Blockers of I_{Kr} are the most widely used drugs for the purpose of prolonging APD [35] and suppress atrial arrhythmias, however, as most I_{Kr} blockers display a "reverse" frequency dependence, their therapeutic effects are limited and the resulting excessive prolongation at lower heart rates has been shown to be proarrhythmic [36, 37]. Compared to I_{Kr} blockers, block of I_{Ks} was hypothesized to be more effective in increasing APDs at short CL in a frequency-independent way [38-44]. On the other hand, during inherited or acquired long QT as a result of application of I_{Kr} blocker, activation of I_{Ks} can compensate for the loss of repolarization current and thus, prevent excessive prolongation of APD and reduce the proarrhythmic risk [38, 45]. Therefore, depending on different pathological conditions, both blockers and activators of I_{Ks} can provide potential effective treatment. In terms of drug development, understanding the effect of I_{Ks} on the dynamics of repolarization of action potential, i.e. restitution and memory, becomes very important. However, little information about these effects is available in the literature. The aim of this phase of the study is to provide the extra piece of

information by determining the dynamics of action potential repolarization during manipulation of I_{Ks}. This is phase 3 of the current study and will be referred as the drug study in the following chapters.

Hypotheses for the current study are: 1) hysteresis in alternans threshold occurs during DI independent pacing mechanisms other than restitution constitute the only underlying mechanisms; 2) regional differences in hysteresis, i.e. memory exists in the pig ventricle and will allow potential identification of the site of arrhythmia initiation; 3) enhancement/minimization of I_{Ks} influence both restitution and memory properties, and these will affect electrical stability. The rest of the dissertation is organized as follows: Chapter II provides electrophysiology background as well current understanding of ventricular arrhythmias and the underlying cellular mechanisms; Chapter III describes the techniques used in the current study; results from the experiments are presented in Chapter IV, followed by the discussion and interpretation of the results in Chapter V. Conclusions and significance of the study will be discussed in Chapter VI, and finally limitations will be discussed in Chapter VII.

Chapter II Background

As mentioned in Chapter I, VT or VF are the leading causes of sudden cardiac death. Sustained re-entrant VT will mostly degenerate into VF [46]. VF is an extremely dangerous life-threatening event, as during fibrillation, the heart muscle contracts in an uncoordinated and random manner and cannot pump blood to the body. Therefore, understanding the underlying mechanism of VF becomes a critical issue in developing effective treatment to suppress or prevent VF. In this chapter, I will start with discussing the major mechanism of VF, i.e. reentry (section 2.1), then introduce currently believed factors that account for reentry at cellular level (section 2.2-2.4), and finally talk about existing antiarrhythmic drugs used to treat different types of arrhythmias (section 2.5).

2.1 Reentry

Initiation of VF has been linked to several different mechanisms [46-50], among which reentry is proposed as the major mechanism that accounts for most lethal cardiac arrhythmias. Reentry, or re-entrant circuit, is defined as an electrical impulse that recurrently travels in a circular pathway within the heart, rather than move from one end of the heart to the other and stop as in the normal conduction of electrical waves in the heart. In a normal heart beat, action potentials of cardiac cells can only be excited once and propagate in one direction because of the refractory period. However, re-entry could occur when there is abnormally prolonged repolarization or prolonged refractory period in a small area of the heart, where the normal propagation fails to excite myocytes in this area, i.e. unidirectional block occurs in this area. If the conduction velocity is slow enough in the adjacent normal tissue to allow the blocked area to repolarize and becomes

excitable, the antegrade pulse can then conduct through this blocked area. Then, if this antegrade impulse travels slow enough to allow the normal area to recover, then it can travel through the normal area again and thus, form a circular pathway for electrical conduction to sustain by itself. A model of initiation of reentry is shown in **Figure 2.1**.

Reentry is a stationary process which can be self-sustained. Transition from the stable reentrant tachycardia into fibrillation is proposed to occur due to spiral wave breakup. Briefly, when there is at least one [51-53] or multiple [54-58] two- or three-dimensional spiral waves present in the heart, collisions among the waves and formation of new child spiral waves with higher frequencies may occur because of different wave lengths and tissue heterogeneities, which add more complexity to the dynamics of these spiral waves and result in chaotic contraction of cardiac muscle, which is, VF. Although the spiral wave breakup theory is believed as the general process for initiation of VF, the exact mechanisms underlying spiral wave breakup have not been clearly understood. Currently, there are several mechanisms related to the breakup of spiral waves, which include electrical activations at cellular level and conduction of electrical signals at tissue and organ level. In the current study, we mainly focus on mechanisms at the cellular level, i.e. dynamics of cardiac action potential repolarization. Before getting into the details, I would like to introduce cardiac action potential and involved ion channels in the following section.

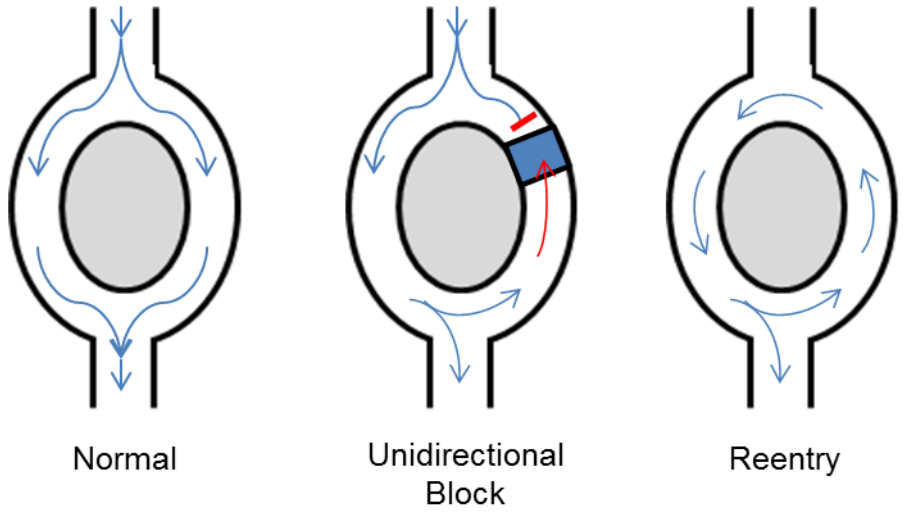

Figure 2.1 A model for reentry.

The figure is a sketch of reentry based on [59]. In normal tissue (left pannel), if there are two conduction pathways (branch 1 and 2), the action potential will travel down each branch and normal action potentials would be recorded by an electrode. Reentry (right panel) can occur if branch 2, has a unidirectional block (middle panel), in which case the conduction velocity reduces in the area and impulses can travel retrograde (from branch 1 into branch 2) but not antegrade. When this condition exists, an action potential will travel down the branch 1, into branch 2, and then travel retrograde through the unidirectional block in branch 2 (red line). When the action potential travels through the block area, if it finds the tissue excitable, then the action potential will continue by reenter the branch 1. Thus, a circular pathway (right panel) of high frequency impulses will become the source of action potentials that spread throughout the region of the heart.

2.2 Cellular Electrical Activity: Cardiac Action Potential

Cardiac action potentials are generated by movement of positive and negative ions through the ion channels on the cardiac cell membranes [60]. When the cell is in diastole and not stimulated the resting membrane potential is about -90 mV [61], and dominated by equilibrium potential of potassium (K^+) current. An action potential is triggered by an electrical signal and can be characterized by a rapid depolarization followed by a relatively slow repolarization back to the resting membrane potential. An action potential has 5 phases (**Figure 2.2**): Phase 0 is the upstroke or rapid depolarization phase which occurs when the cell is stimulated by an electrical signal that crosses a threshold which opens the fast sodium (Na^+) channel. Opening of Na^+ channels causes a rapid influx of Na^+ ions, bringing the intracellular potential to about +10 mV, which is close to the equilibrium potential of Na^+ current (~ 50 mV). Phase 1 is the initial repolarization phase, or "notch" of the action potential, which is caused by the inactivation of the fast sodium channels and transient outward flow of the potassium current I_{to1} and I_{to2}. A plateau phase, i.e. phase 2 of an action potential is formed by the balance flow of several ion currents across the cell membrane. Dominant among these are inward flow of calcium (Ca^{2+}) current through L-type channels and outward flow of K^+ current through I_{Ks}. In addition, sodium-calcium exchanger current (I_{NaCa}) and sodium potassium pump current (I_{NaK}) also play a minor role in this balance. After close of the L-type calcium channels, rapid repolarization, i.e. phase 3 of an action potential starts to occur as the net outward current caused by the still opening I_{Ks} channels brings down the membrane potential and thus, allows opening of other potassium channels, such as rapid and slow delayed rectifier current (I_{Kr} and I_{Ks}) and inward rectifier current (I_{K1}). When the membrane

potential repolarizes to about - 80 ~ - 85 mV, I_{Kr} and I_{Ks} channels close, while I_{K1} channels remain open throughout phase 4 to maintain resting membrane potential. **Figure 2.2** shows a schematic of the depolarizing and repolarizing currents during a cardiac action potential. Also shown in the figure are two critical measures for the current study: 1) APD, i.e. action potential duration, defined as the duration of action potential, an equivalent to the contraction time, including phase 0 to phase 3; 2) DI, i.e. diastolic interval, refers to the duration when transmembrane potential is at resting level (~-90 mV), or phase 4. Relationship between the two, i.e. APD and DI, and their role in arrhythmia generation, will be discussed in the next section.

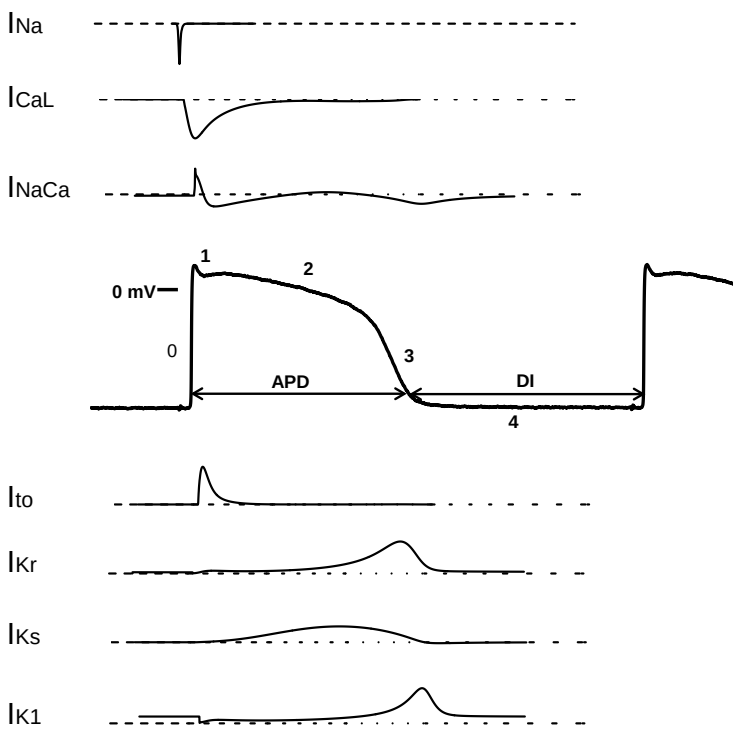

Figure 2.2 Schematic of ion currents during cardiac action potential.

Figure shows the depolarizing (above the action potential) and repolarizing (below the action potential) currents that underlie the cardiac action potential in mammalian ventricle. Dotted lines represent baseline (current is 0), upward/positive/deflection indicates inward current while downward/negative indicates outward current. I_{K1} is known as the inward rectifier current. APD: action potential duration; DI: diastolic interval.

2.3 Dynamics of Action Potential Repolarization: Restitution and Memory

Cardiac electrical stability describes the propagation of electrical activations throughout the heart. Loss of cardiac electrical stability can induce abnormal dynamics of action potential repolarization that can lead to arrhythmia. Alternans of APD, i.e. beat-to-beat variation in APDs, is one of the most important abnormal behaviors of electrical activation, which has been proposed as a precursor of arrhythmia generation [9]. There are two forms of alternans: concordant alternans, where alternans remain in the same alternating pattern in the heart, and discordant alternans, where alternans with long-short-long pattern in one area of the heart transits into short-long-short in another. Spatially discordant alternans has been linked to spiral wave breakup and initiation of reentry in previous studies using computational modeling [6, 62]. Therefore, understanding the mechanisms of onset of alternans is critical in exploring the mechanisms for VF. Restitution of APD and cardiac memory are proposed to be two dominant factors.

Restitution Hypothesis

For decades, the electrical restitution hypothesis has been believed to predict the occurrence of alternans and its transition into arrhythmias and VF [15, 17, 18, 63-66]. Electrical restitution theory was first raised by Nolasco & Dhal in 1968 where they plotted the current APD with respect to its preceding DI [67]. The curve obtained is called the APD restitution curve. **Figure 2.3** shows an example of restitution curve recorded during a pig experiment. The slope of the restitution curve at certain DI value was then used as a major predictor for occurrence of APD alternans. Note that the

restitution slope is close to a flat line, i.e. slope close to 0, during long DIs, or slower heart rate, and it steepens sharply as DI/CL decreases. According to the restitution hypothesis, the slope of the restitution relationship could determine whether a disturbance of CL will lead to APD alternans and conduction block. A shortening of DI due to a premature heart beat will shorten the APD for the next beat and lengthen the DI for that beat (given that CL=APD+DI), which in turn generating a long APD for the next beat, leading APDs to oscillate in a short-long-short pattern. This process in evolution of APD after a disturbance of CL is shown in **Figure 2.4**. Note that at fast pacing rate, or short CL, the restitution curve can be simplified to a straight line with a constant slope, as shown in the figure.

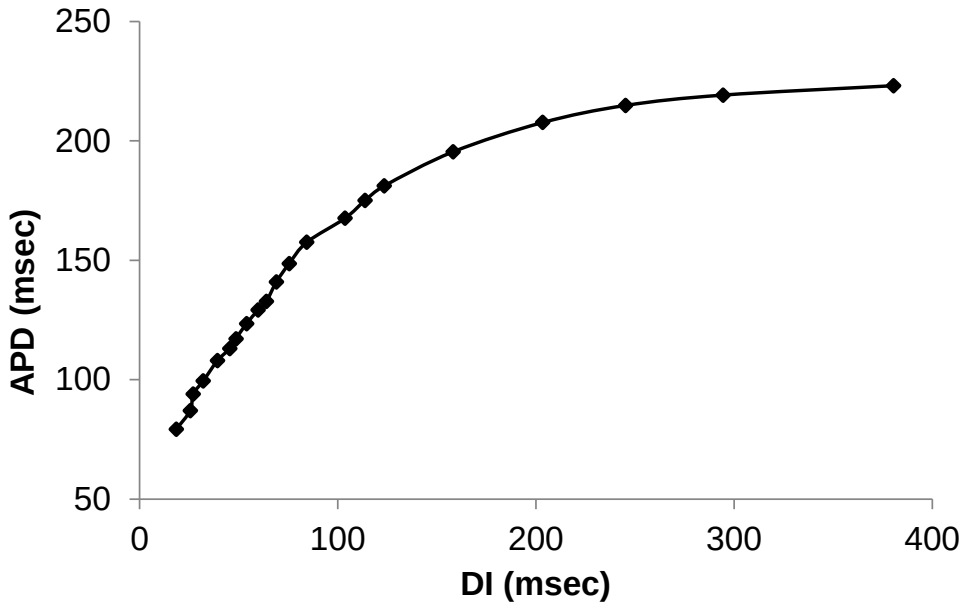

Figure 2.3 Example of restitution curve recorded from pig ventricular tissue.

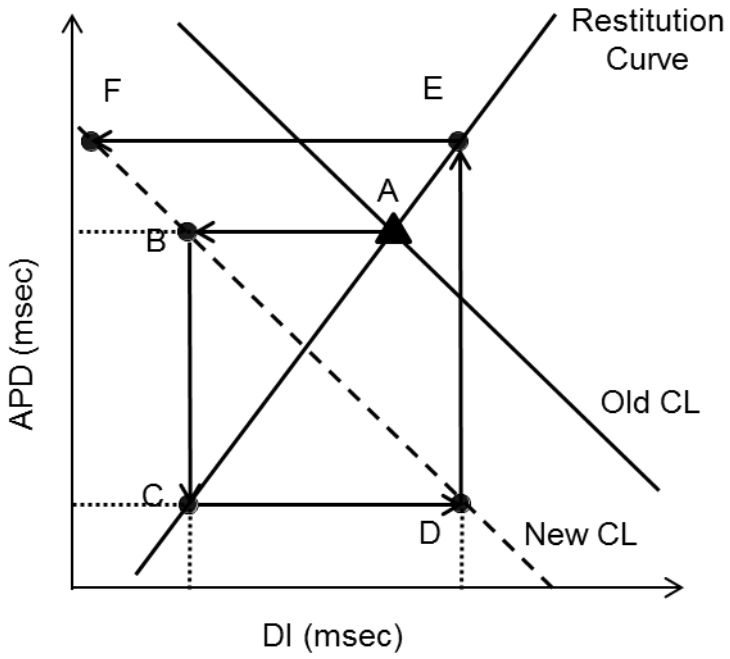

Figure 2.4 Evolution of APD during CL disturbance in restitution hypothesis.

The figure shows APD evolution when CL is shortened from an old CL to a new CL. The original operating point was at the intersection of the old CL and the restitution curve (simplified to a straight line), i.e. point A. When CL is reduced, the DI for the next beat is determined by point B, as DI=CL-APD (in this case the next DI decreases). Then the following APD is determined by the restitution curve and appears at point C. Similarly, the next DI and its following APD can be obtained at point D and E. Depending on the slope of the restitution curve, the evolution can diverge and lead to a functional block (slope > 1), or converge to a new operating point (slope < 1), or it will form a closed loop (slope = 1) in which case APD oscillates between two values, i.e. alternans.

Figure 2.5 shows an example of simulated APD traces during a disturbance of CL at different restitution slopes. As shown in **Figure 2.5**, if the slope < 1, the oscillation will attenuate and the heart rhythm will stabilize to a new steady state; however, if the slope > 1, the amplitude oscillation will increase beat after beat, eventually leading to conduction block and reentrant arrhythmia [68]. When slope = 1, alternans of APD will have a constant amplitude. In this case, APD alternates between two steady states, without block or attenuation. Note that **Figure 2.5** was not obtained during experiments. It was generated by duplicating one action potential recorded from pig ventricular tissue. The duration and amplitude of each action potential were manipulated according to the predicted values based on the relationship that $APD_n + DI_n = CL$, and the restitution relation between APD and DI, i.e. $APD_n = s \cdot DI_{n-1}$, where s represents the slope of restitution. The rational of manipulating both duration and amplitude of action potential is that previous studies [6, 33, 47, 69] have shown that both measures are affected by the change of DI, however, in the current study, the main focus is on duration of action potential, i.e. APD.

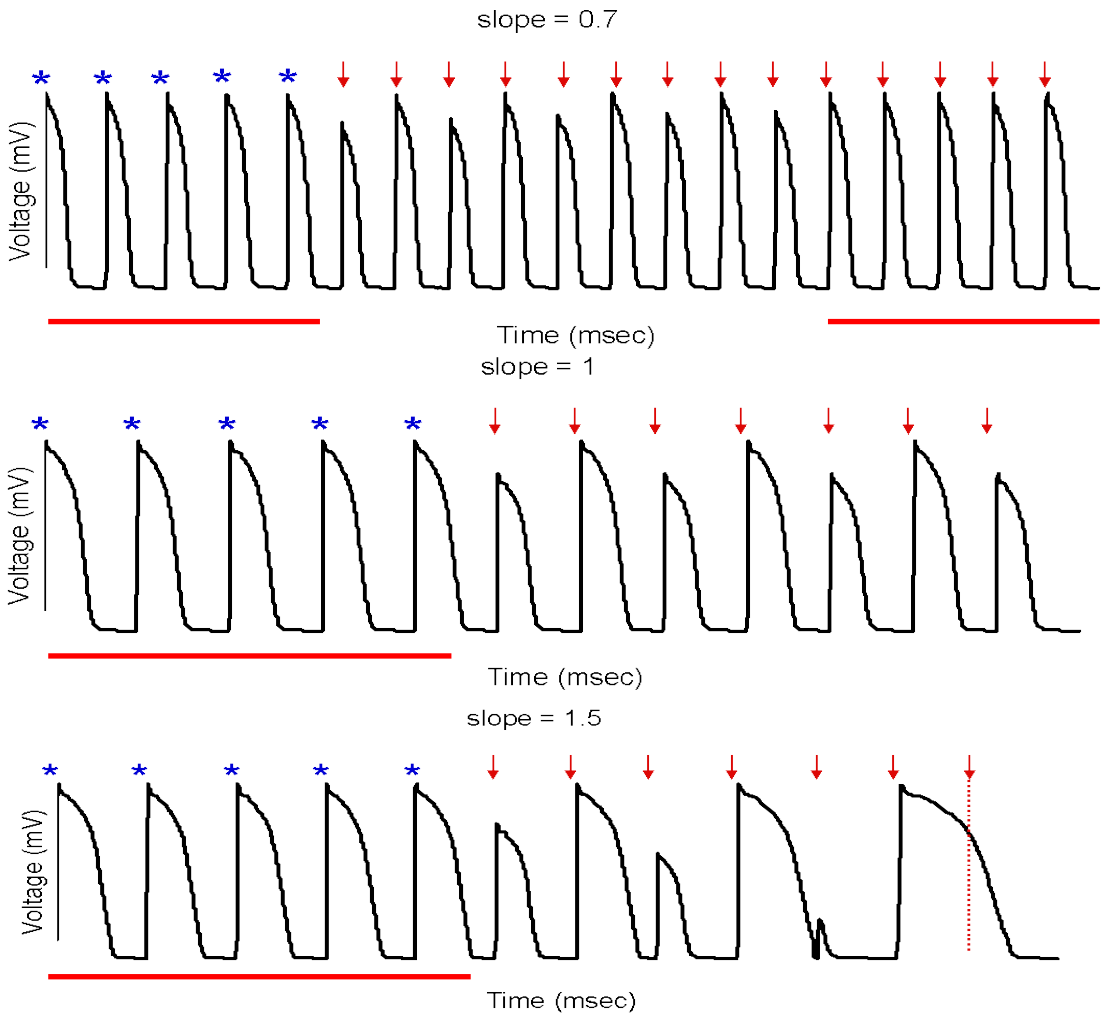

Figure 2.5 Simulated APD changes with different restitution slopes during CL disturbance.

Note: the action potentials are simulated traces shown as a schematic. Action potentials with blue stars represent normal activation at original CL. Action potentials with red arrows represent activations at a new CL. Action potentials with underlying red lines are identical, i.e. they are at the steady state with no changes in APD.

Two Forms of Restitution: Standard and Dynamic Restitution

There are two widely used pacing protocols to determine the restitution relationship: standard and dynamic protocols [64]. In the standard (S1-S2) protocol, an extra stimulus (S2) is delivered after steady state (usually after 20 beats) is achieved under basic cycle length (BCL) pacing (S1). By progressively decreasing the S1-S2 interval until block occurred, the relationship between the APD after the S2 stimulus and the DI before the S2 stimulus is determined as the standard restitution. However, in most cases, investigators report a slope of the standard restitution smaller than 1 [14, 70], even when alternans were observed. Assuming that lack of information about rapid accumulation and dissipation of memory in standard restitution is responsible for the discrepant result [14], the dynamic protocol is introduced. In the dynamic protocol, the heart is paced at a fixed CL until steady-state is obtained, and the pacing CL is decreased to achieve a new steady-state. The process is repeated until block occurs. The APD and DI from the last beat of every CL, i.e. the steady state response is used to determine the dynamic protocol, therefore, it is also called steady-state restitution [12]. Dynamic restitution has been shown to result in a steeper slope than standard restitution and thus, the slope of dynamic restitution is suggested to be accounted for APD dynamics during VF [64]. A few studies have shown that VF could be suppressed by flattening the restitution curve [66, 71]. For example, Riccio et al. has shown that drugs that flattens restitution slope, e.g. verapamil, prevents the induction of VF or turn VF into periodic rhythms, while drugs that does not reduce restitution slope, e.g. procainamide, does not prevent or regularize VF.

However, despite of the limited success during experimental studies, most recent studies suggest that restitution relation alone is not adequate to predict alternans, and that it is

necessary to consider the rate-dependent characteristics of restitution and the existence of cardiac memory [23, 72]. In a previous study by our group, we used a feedback based DI protocol to pace cardiac tissues at constant DI for each action potential, and persistent alternans was observed independent of the change of DI. These results confirmed that there exist mechanisms that are independent of restitution relationship but also affect electrical stability. One example of these restitution independent mechanisms is cardiac memory.

Cardiac Memory

Cardiac memory is defined as the dependence of APD on previous APDs and DIs in a time scale of several seconds to minutes. **Figure 2.6** shows an example of cardiac memory recorded during a pig experiment. The figure shows that there is a delay between peak values of DIs and the resulting APDs, demonstrating the existence of memory. Besides electrical restitution, cardiac memory is proposed as another potentially important mechanism underlying electrical arrhythmia. APD adaptation or accommodation has been reported as a very common phenomenon during constant CL pacing in many studies [14, 73-75]. Using a less known constant CL protocol, Tolkacheva et al. [76] claimed the existence of a fast and slow component of memory during CL adaptation, where the short-term memory was reported in a two-dimensional model [14]. In addition, cardiac memory has been implicated in the hysteresis of alternans during increasing and decreasing CL pacing, i.e. after initiation, alternans persisted to longer CL than the threshold CL [23, 25, 77]. In our previous studies [17, 78], the memory effect has been quantified using a feedback-based DI protocol where DI changes in a sinusoidal pattern. The resulting APD trace showed similar pattern but with

asymmetric phase delay during descending and ascending phases of DI, which we refer to as hysteresis in restitution.

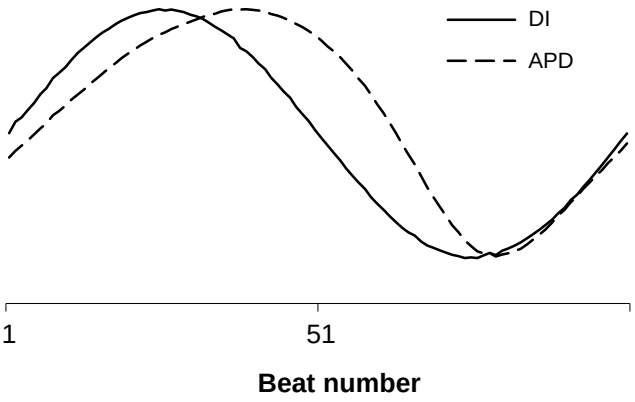

Figure 2.6 Example of cardiac memory.

The delay between the peaks of the sinusoidal DI trace (solid line) and the resulting APD trace (dashed line) indicate the existence of memory effect, i.e. when DI starts decreasing from its peak value, APD still increases for a few beat. Data was obtained from a pig study. Note that the DI and APD values are scaled and vertically shifted to facilitate illustration of the delay.

Role of Memory in Electrical Stability

Memory has been hypothesized to have a stabilizing effect on electrical activation [15, 18, 19, 33]. **Figure 2.7** shows the schematic of iteration of changes in APD and DI produced by a change in CL to provide a possible mechanism for the stabilizing effect of memory. Panel A shows iteration of a disturbance predicted by a conventional restitution curve with slope > 1 leads to increasing oscillations of APD and DI, and eventually results in the APD being longer than the new CL, so that the next stimulus would occur in the refractory period of the AP which leads to block. However, as shown previously, when memory is taken into account, the restitution follows two trajectories depending on the direction of change in DI, specifically, the APD trajectory during increasing DIs is located below that of the one during decreasing DIs. Panel B shows the same iteration of disturbance, but with two trajectories (i.e. hysteresis) as described above, that is, when memory is present. The figure shows that memory has a dampening effect on the disturbance and thus increases stability. When hysteresis is present, a disturbance does not always have to result in APD oscillations until either a stable point or block is reached. Note that the iteration of disturbance in the restitution hypothesis and iteration with memory are both predicted values using theoretical models and not related to experimental results.

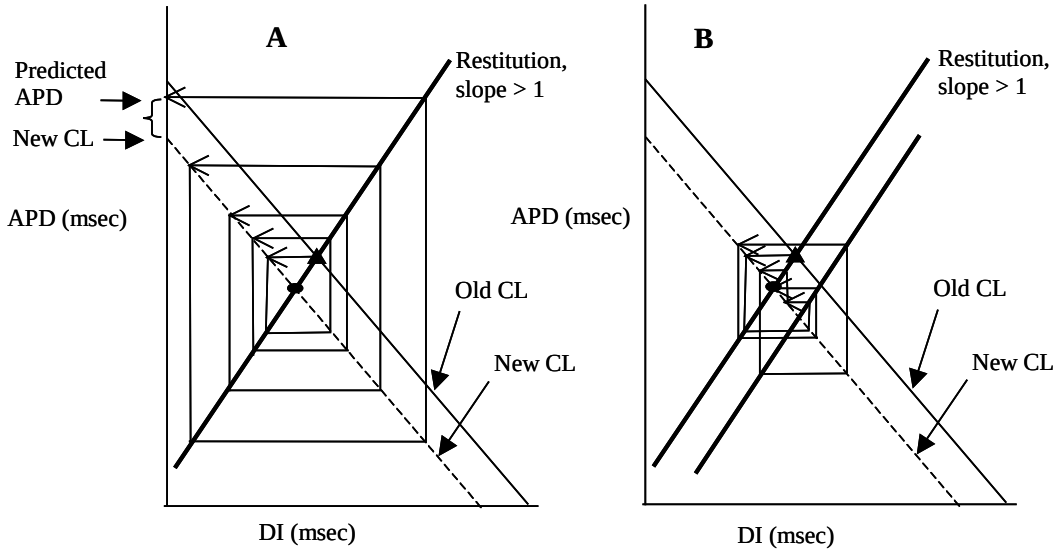

Figure 2.7 Iteration of APD during disturbance in CL with/without memory.

The figure shows APD evolution similar to that explained in **Figure 2.4**. A: Iteration of APD based on simplified restitution curve with a slope > 1. When CL was decreased from old CL to new CL, block was induced after successively increasing APD alternation. B: Iteration of APD with the same slope >1 but with presence of memory. Block was not induced in this case as oscillations in APDs are dampened by the existence of memory. The figure shows that with the presence of memory, APD following a longer DI does not necessarily increase.

2.4 Ionic Mechanisms for Restitution and Memory

Ionic Mechanism for APD Restitution

Previous studies suggested that the rapid delayed rectifier potassium current (I_{Kr}, **Figure 2.2**) may contribute importantly to dynamics of action potential repolarization [16, 79, 80]. The contribution of I_{Kr} to repolarization alternans has been discussed in details by Hua et al.[80]

Slow deactivation is one of the most prominent characteristics of I_{Kr}. The deactivation time constants of I_{Kr} at -85 and -70 mV are about 35 to 50 msec, which are slow enough to prevent complete deactivation of I_{Kr} at short CLs where the DIs are also short. A disturbance in CL, i.e. a sudden decrease in CL leads to instant shortening of DI, and incomplete deactivation of I_{Kr}. These non-deactivated I_{Kr} channels get accumulated to the next beat and lead to a bigger peak I_{Kr}, which in turn accelerates the repolarization, and produces a short action potential. As the DI following the short APD is longer, deactivation of I_{Kr} is more complete and no accumulation occurs for the following beat, repolarization slows down and produces a long action potential. **Figure 2.8** shows a figure of APD alternans and the related I_{Kr} current.

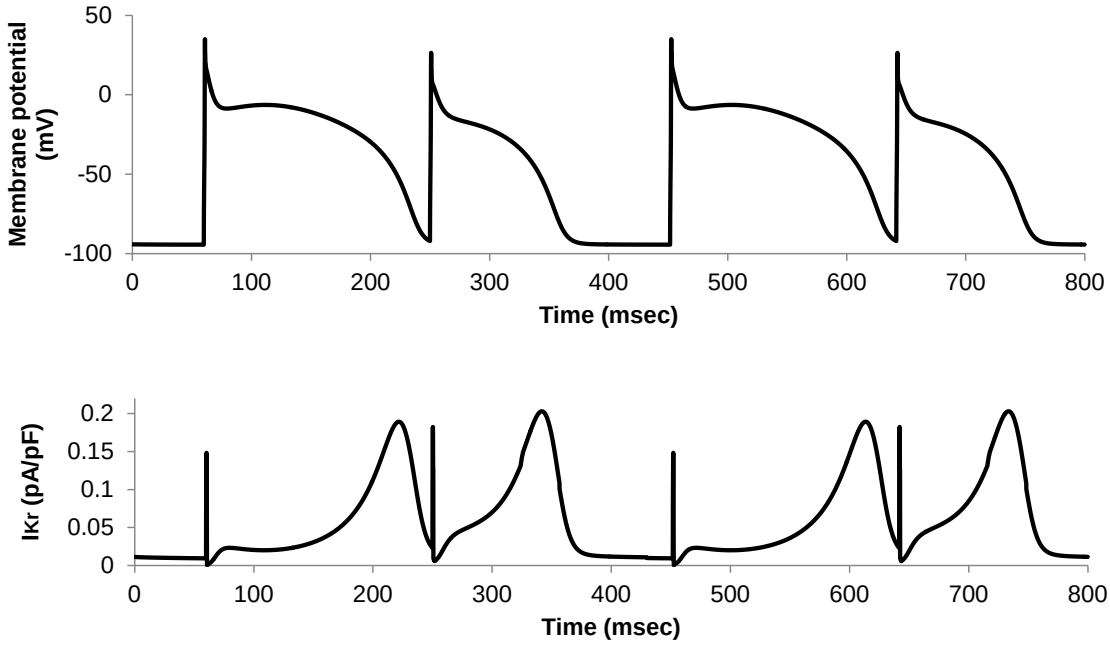

Figure 2.8 Transmembrane potential and I_{Kr} during APD alternans.

During APD alternans, peak I_{Kr} is larger during the shorter action potential, because the short action potential is preceded by a short DI, during which deactivation of I_{Kr} may have been incomplete, resulting in a fraction of channels being activated before the onset of the short action potential. The incomplete deactivation also accounts for the slightly elevated baseline I_{Kr} during the short DI.

Ionic Mechanism for Cardiac Memory

Calcium cycling has been hypothesized to be a contributing factor for the hysteresis, i.e. memory effect as shown in our previous study [78]. In detail, the amount of intracellular calcium (Ca_i) is larger during the DI descending phase than the ascending phase (**Figure 2.9**C). This difference occurs because, during the descending phase, each activation is

preceded by a longer DI, providing more recovery time for calcium, and thus higher Ca stores in the sarcoplasmic reticulum (SR). This increase in the SR calcium causes an increased release during calcium induced calcium release (CICR), and thus leads to an increased Ca_i. The increased Ca_i, in turn, increases the APD during descending phase (**Figure 2.9**B, point B). Opposite happens during the ascending phase and results in a short APD (**Figure 2.9**B, point A). Thus, it is the asymmetry in Ca_i concentrations that leads to a difference in APD at the same DI value (beat 100 and 150) resulting in the hysteresis loop.

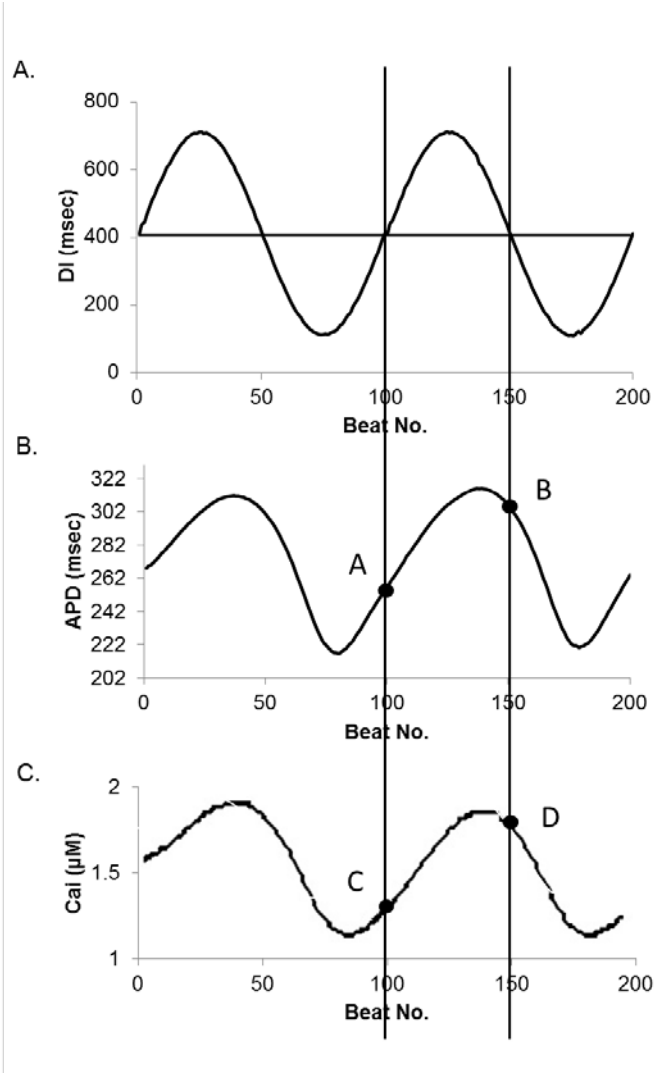

Figure 2.9 Intracellular calcium cycling during sinusoidal DIs.

A: Sinusoidal DI trace with 400 msec center DI. B: APD trace resulted from the DI trace in panel A. C: A sketch of intracellular calcium cycling during sinusoidal DI sequence based on our previous study [21].

2.5 Antiarrhythmic Drugs

Given the prevalence of arrhythmic problems, it becomes urgent to develop efficient antiarrhythmic therapies. Antiarrhythmic drugs are widely used as a pharmaceutical treatment for suppression of different types of life-threatening arrhythmias. Most antiarrhythmic drugs are grouped into 4 main classes according to Vaughan Williams classification method, based on their dominant cellular electrophysiological effect, or, the primary mechanism of its antiarrhythmic effect. The class I antiarrhythmic agents interfere with the Na^+ channel. Class I agents are further divided into three subgroups IA~IC based on their effect on APDs. Class II agents are conventional beta blockers, which decrease the effects of sympathetic activity on the heart. These agents are particularly useful in the treatment of supraventricular tachycardia as they decrease conduction through the AV node. Class III agents predominantly block K^+ channels, thereby prolonging repolarization. Conduction velocity is not affected since these agents do not affect the Na^+ channel. The prolongation of APD and refractory period, combined with a normal conduction velocity, could prevent re-entrant arrhythmias. Class IV agents are Ca^{2+} channel blockers. They decrease conduction of activation from the SA node and shorten the plateau phase of the cardiac action potential and thus shorten repolarization. They also reduce the contractility of the heart, so these are inappropriate in heart failure. There are other agents which work through mechanisms that are different from class I~IV agents. These agents are sometimes referred as “Class V” agents.

However, drug treatment has been questioned for its efficacy and safety [81]. It has been shown that although antiarrhythmic drugs could have potential antiarrhythmic benefit such as terminating sustained tachycardia and alleviate symptoms related to chronic

arrhythmia, side effects of these antiarrhythmic drugs can be substantial and can increase proarrhythmic risks and mortality rate [81]. For example, Class III drugs, which are mostly I_{Kr} blockers, have been shown to induce torsades de pointes [82-84], a polymorphic VT characterized by a twisting QRS complex in ECG. Torsades de pointes is associated with prolonged QT interval and can progress to VF. Therefore, new therapies which minimize the proarrhythmic risk, or drugs with higher benefit to risk ratio need to be developed.

Chapter III Methods

3.1 Tissue Preparation

All animal related studies were approved by the Institutional Animal Care and Use Committee at the University of Kentucky. Farm pigs weighing 18-21 kg were used for data collection. For the heterogeneity study, 15 pigs were used, of which 6 were also used to study the hysteresis in alternans threshold. Another 7 pigs were used to study the effect of I_{Ks} Changes.

In all experiments, pigs were sedated using a combination of Telazol (4-8mg/kg), Ketamine (2-4mg/kg), and Xylazine (2-4mg/kg). Pigs were then anesthetized by thiopental sodium (Pentothal, 10-11mg/kg, IV) for phase 1 and 2 of the study, or by sodium pentobarbital (30–50mg/kg, IV) for phase 3. After anesthesia, hearts were rapidly excised and placed in chilled modified Tyrode's solution. Composition of the solution (in mmol/L) was: 0.5 $MgCl_2$, 0.9 NaH_2PO_4, 2.0 $CaCl_2$, 137.0 NaCl, 4.0 KCl and 5.5 Glucose. To the gassed solution, $NaHCO_3$ was added until the pH was obtained to be between 7.3±0.05.

Tissues from left ventricles were used to collect data for investigating hysteresis in alternans threshold (phase 1). For heterogeneity study (phase 2), epicardial and endocardial tissue slices approximately 20×10×5 mm were excised from the mid to apical anterior-lateral region of both left and right ventricular free wall [28, 85] and mounted in plastic chambers. For the I_{Ks} study (phase 3), two tissue slices were excised adjacent to each other from the antero-lateral region of the right ventricular free wall, one for agonist

and one for antagonist. All preparations were superfused by oxygenated (95% O_2 plus 5% CO_2) modified Tyrode's solution warmed to 36±1˚C.

All tissue preparations were paced at basic cycle length (BCL) of 500 msec for equilibration. Recordings were not started until the tissues were equilibrated for about 2 to 3 hours for endocardial and 4 to 6 hours for epicardial preparations, similar to equilibration times reported by others in canines [85].

3.2 Data Acquisition

Experimental Setup: Figure 3.1 shows a schematic representation of the experimental setup. The tissue was paced by bi-polar platinum-iridium electrodes. Transmembrane potentials were recorded by machine pulled glass microelectrodes. After amplification by an intracellular amplifier (Model 3100, A-M Systems Inc.), the signal was sent to two different pathways. On one hand (left side of **Figure 3.1**), the signal was digitized using a commercial data acquisition system (DI-720, DATAQ Instruments) and stored in computer memory. Sampling rate was 10,000 samples/second for phase 1-2 of the study and 50,000 samples/second for phase 3. Note that 50, 000 samples/second was chosen for recording another parameter that is not related to the current study, and that 10, 000 samples/second is adequate for the current study. On the other hand (right side of **Figure 3.1**), the amplified signal was digitized and sent to a real time analysis program. The program determined the timing for the next stimulus and sent a digital trigger to the stimulator (Model 2100, A-M Systems Inc.), which delivered a bi-phasic stimulus to the tissue through bi-polar pacing electrode. Duration of the pacing stimulus was 3 msec and

the amplitude was 4 to 6 times diastolic threshold (minimum current needed to produce an action potential).

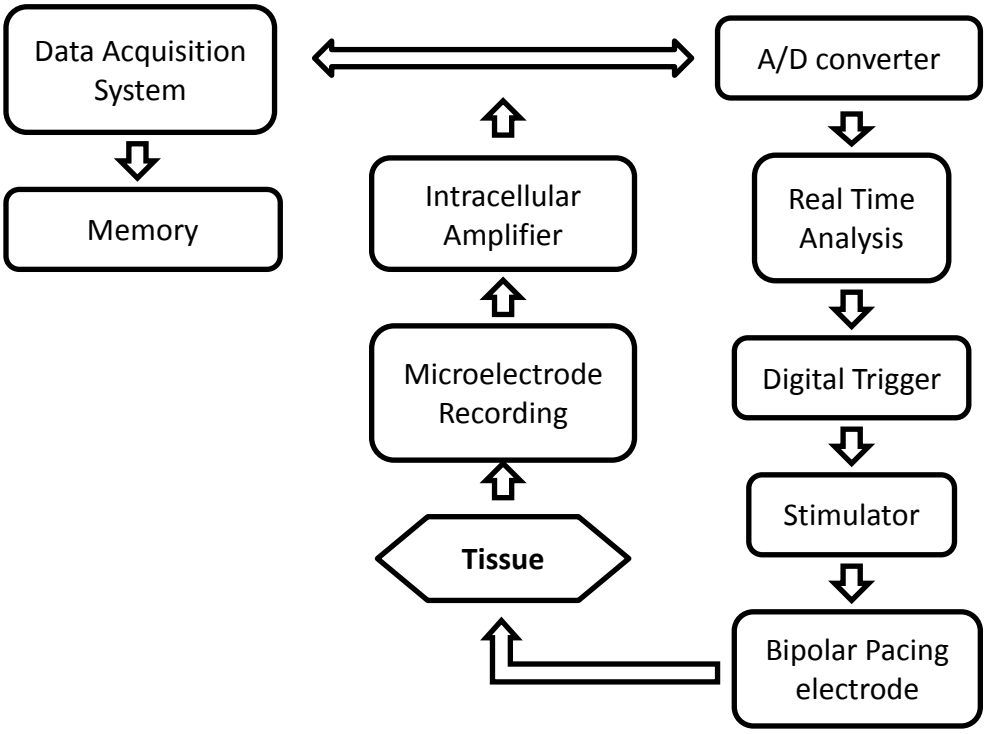

Figure 3.1 Schematic representation of the experimental setup.

Microelectrode recording: After equilibration, the intracellular potentials were recorded at locations close to the pacing electrodes using machine pulled glass capillary microelectrodes filled with 3 Mol KCl. Tip of the microelectrode was < 1 μm, and the resistance was between 10 - 40 MΩ. A reference Ag/AgCl electrode was placed in the corner of the tissue chamber, submerged in the buffer but not contacting the tissue. All measured potentials were the potential differences between the recording electrode and the reference electrode. When the recording electrode was in the bath, the potential was adjusted to be equal to zero by removing any DC offset, as the electrode began impaling the myocyte, a potential drop was seen and the potential decreased from around 0 mV to about -75 mV, i.e. resting membrane potential for cardiac myocytes in a pig. When the impaled myocyte was dying or the electrode moved out of the myocyte, the potential came back from -75 mV to the zero potential. For all experiments, protocols were not started unless the transmembrane potential was stable for at least 5 minutes, i.e. shape and amplitude of the action potential didn't change for 5 minutes. **Figure 3.2** shows an example of the potential changes when the electrode impales the myocyte (A) and comes out of the myocyte (B).

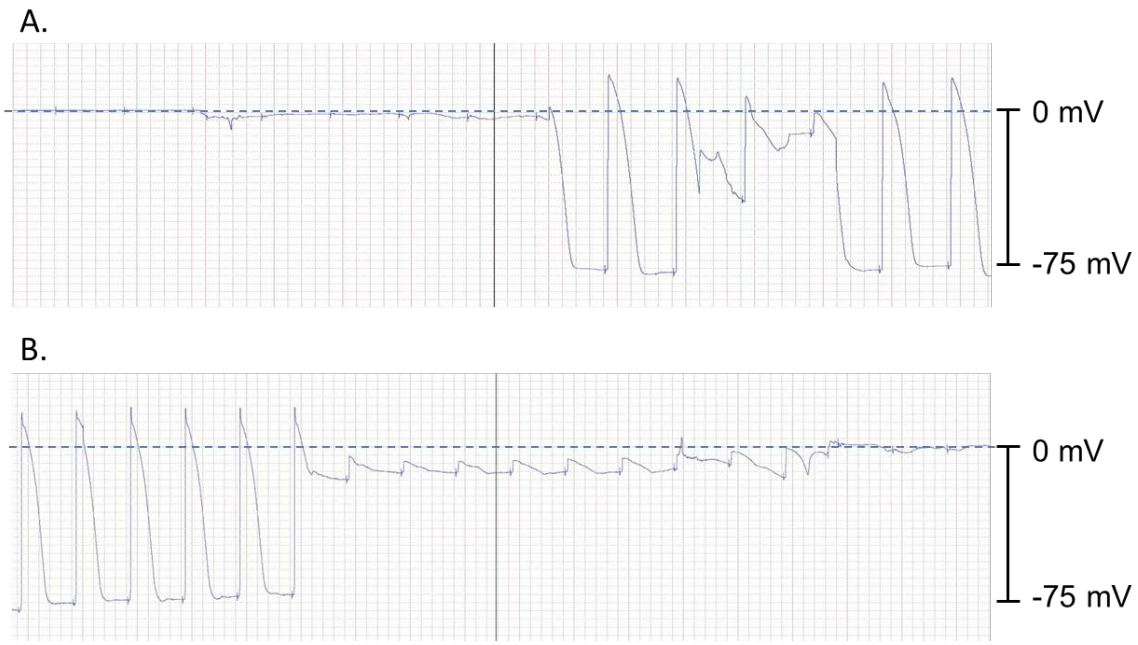

Figure 3.2 Potential changes when entering and exiting the myocyte during microelectrode recording.

Real time DI control: To explore other existing mechanisms underlying APD alternans except restitution, we need to eliminate the restitution effect by minimizing change of DIs. A feedback-based pacing protocol, as described before [15, 21, 86], was used for pacing such that the DIs were explicitly controlled in real-time. Briefly, the time when the cell repolarizes 90% from peak to resting potential was detected in real time by a custom written program, from then the program waited for a predetermined interval before delivering the next pacing stimulus. The predetermined interval became the DI for the next action potential. An illustration of this process is shown in **Figure 3.3**.

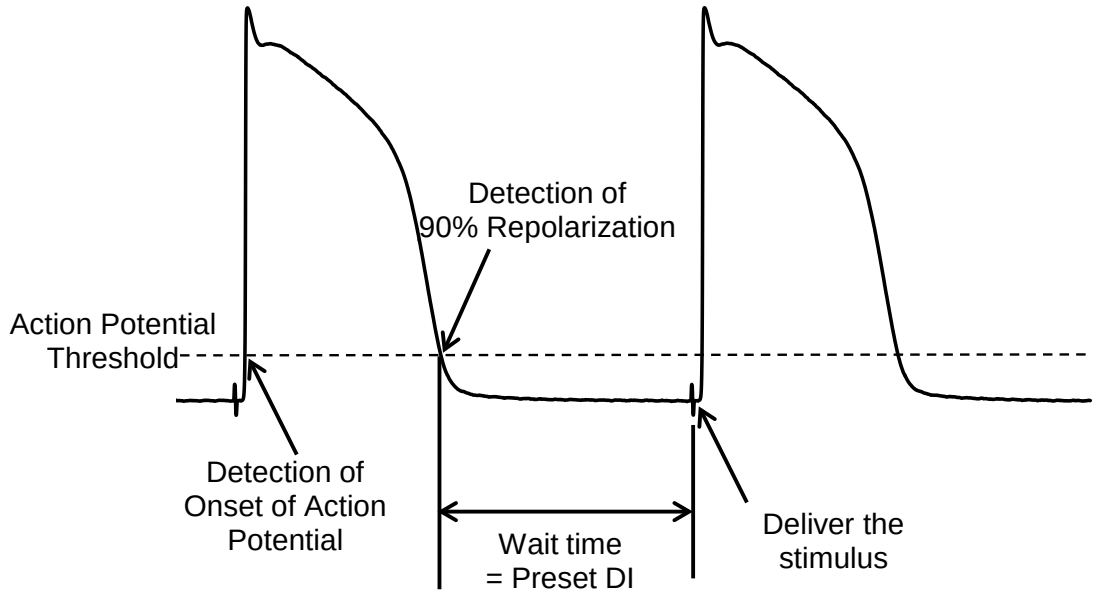

Figure 3.3 Illustration of real time DI control.

The program first detects the onset of an action potential once the transmembrane potential crosses the threshold, which is a preset value calculated as 90% of the amplitude of the action potential. Then the program waits until the transmembrane potential drops below the threshold. This time point was considered as end of an action potential, from which the program waits for an amount of time equal to the predetermined DI value, and then delivers the next stimulus. The time delay from detection of the end of the action potential to delivery of the stimulus is < 0.2 msec.

3.3 Pacing Protocols

Stepwise DI Protocols

Two feedback-based pacing protocols were used to determine the thresholds for onset and termination of alternans. **Figure 3.4** shows an example of the stepwise DI pacing protocol. In both stepwise protocols, DIs decreased first from 50 to 20 msec in steps of 10 msec, and then increased back to 50 msec with the same step change.

Protocol 1.1 30 beats stepwise DI protocol: The tissue was paced for 30 beats at each level of DI. (**Figure 3.4**, thick line)

Protocol 1.2 15 beats stepwise DI protocol: The tissue was paced for 15 beats at each level of DI. (**Figure 3.4**, thin line)

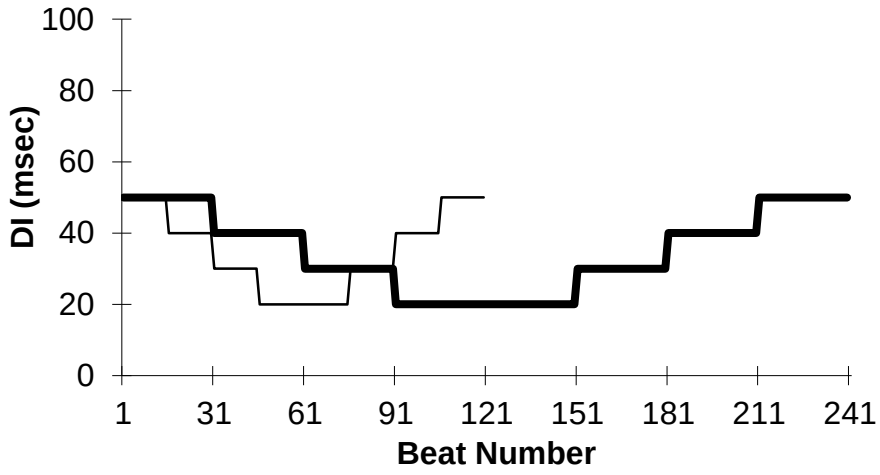

Figure 3.4 Illustration of stepwise DI protocols.

The figure shows the target traces of DI for 30 beats (thick line) stepwise DI protocol (protocol 1.1), and for 15 beats (thin line) stepwise DI protocol (protocol 1.2).

Restitution Protocols

To obtain restitution curves, we used standard (S1S2) and dynamic protocols similar to that previously described by Gilmour et al [12].

Protocol 2.1 Standard Protocol: In the standard protocol, a concurrent S2 stimulus was delivered after every 20 S1 stimuli and the period between S1 and S2 was progressively decreased. The S1S1 interval used in this study was 300 msec and S1S2 interval decreased from 600 msec to 300 msec in step of 50 msec, and then from 300 msec to 200 msec with step of 20 msec. For S1S2 < 200 msec, the decrement was 10 msec until S2 failed to produce an action potential. An example of standard protocol is shown in **Figure 3.5**. The rational for using 300 msec S1S1 interval was because this is the shortest CL which produce a normal 1:1 rhythm without inducing any kind of arrhythmias, i.e. alternans or block. Note that the pigs used in the current study were relatively young (~2 months) with a faster heart rate of ~120 beats/minute.

Protocol 2.2 Dynamic Protocol: In the dynamic protocol, CL decreased from 600 msec progressively with the same decrement as used in standard protocol until block occurred. **Figure 3.6** shows an illustration of dynamic protocol.

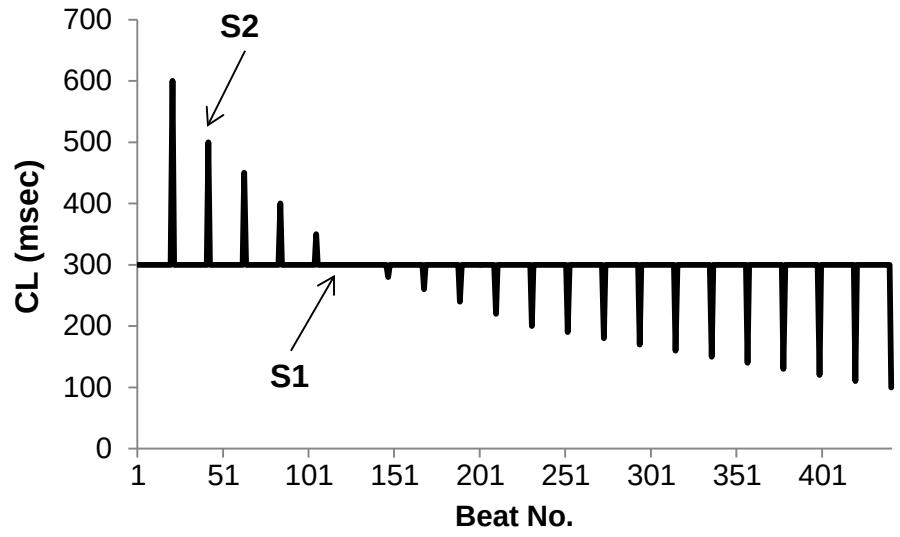

Figure 3.5 Illustration of Standard Protocol.

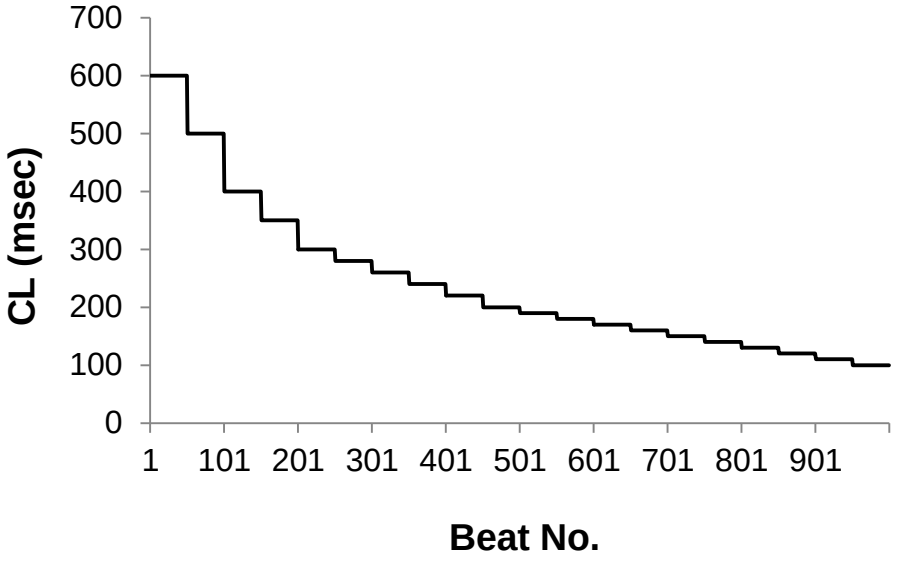

Figure 3.6 Illustration of dynamic protocol.

Sinusoidal DI Protocols

To quantify memory in restitution, two feedback-based pacing sequences with oscillatory changes in DIs were used. In these sequences, DIs oscillated sinusoidally between a maximum and minimum DI around a mean value of DI with a period of 100 beats.

Protocol 3.1 400 msec sine DI protocol: DIs oscillated around a mean DI equal to 400 msec with oscillation of ± 300 msec, i.e. DI ranges from 100 msec to 700 msec. (**Figure 3.7**)

Protocol 3.2 150 msec sine DI protocol: DIs oscillated around a mean DI equal to 150 msec with oscillation of ± 140 msec, i.e. DI ranges from 10 msec to 290 msec. (**Figure 3.7**)

In both protocols we paced the tissue for two complete cycles, preceded by 20 beats of constant pacing at a DI equal to the mean DI of the protocol in order to minimize transition effects induced by switching from 500 msec CL pacing to DI control pacing. An example of the sinusoidal DI sequence is shown in **Figure 3.7**. Each protocol was run two to three times. Between trials, tissues were paced at CL of 500 msec.

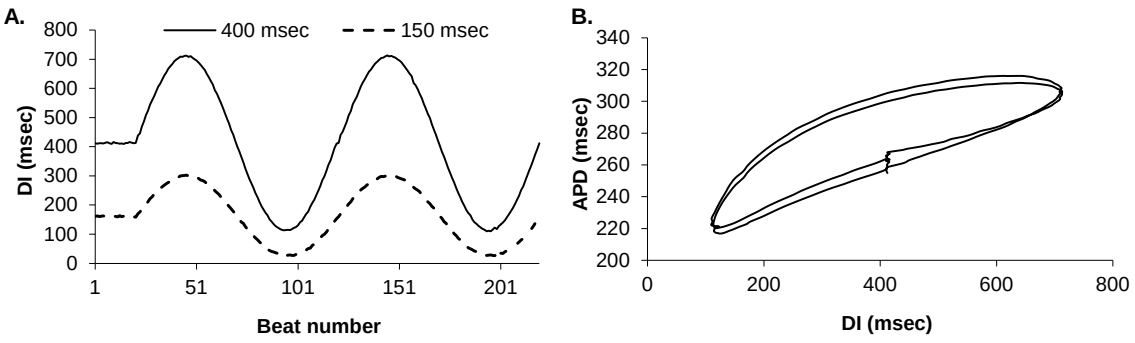

Figure 3.7 Example of sinusoidal DI protocols.

A: An example of the 400 msec and 150 msec sinusoidal DI protocols, with 20 beats of DIs at center value followed by 2 cycles of sinusoids. B: The restitution relationship between APD and DI obtained from the 400 msec DI protocol shown in panel A, which shows two complete hysteresis loops after 20 beats adaptation at center DI (400 msec).

Constant CL/DI Protocols

To explore the existence of APD alternans during DI dependent and independent mechanism, constant CL/DI protocols were used to produce alternans.

Protocol 4.1 Constant CL protocol: CLs were held constant for all beats in a trial. To produce alternans, pacing CLs were ≤ 300 msec and were progressively reduced between trials until block occurred.

Protocol 4.2 Constant DI protocol: DIs were kept constant for all beats in a trial. DIs ≤ 40 msec were used to produce APD alternans.

Protocols used in Each Phase of the Study

In phase 1 of the study, stepwise DI protocols (protocol 1.1-2, **Figure 3.4**) were used to determine the existence of hysteresis in alternans threshold. The rationale of using two different step sizes is that compared to the 30 beats stepwise protocol, memory accumulation would be less in the protocol with 15 beats in each step. Therefore, hysteresis in alternans threshold would be different if memory plays a role in the hysteresis.

In phase 2 of the study, heterogeneity in memory was investigated by quantifying hysteresis in restitution using sinusoidal DI protocols (protocol 3.1-2, **Figure 3.7**). In order to facilitate comparison with studies in the literature, restitution curves were obtained in two samples for each, i.e. the left and right, endocardial and epicardial tissues using standard (**Figure 3.5**) and dynamic (**Figure 3.6**) protocols. However, the objective was to quantify heterogeneity in expression of memory and not restitution of APD per se. S1S2 interval started from 400 msec for these two experiments. To investigate the existence of DI dependent and independent mechanisms of APD alternans, constant CL and constant DI protocols (protocol 4.1-2) were also conducted in a few animals.

In phase 3 of the study, to study the effect of I_{Ks} manipulation on restitution, standard and dynamic restitution curves (protocol 2.1-2, **Figure 3.5** and **Figure 3.6**) were obtained in all animals before and after application of drugs. To study the effect of I_{Ks} changes on memory, sinusoidal DI protocols (protocol 3.1-2, **Figure 3.7**) were conducted. Constant CL/DI protocols (protocol 4.1-2) were conducted to explore the effect on alternans occurrence before and after application of drugs.

3.4 I_{Ks} Agonist and Antagonist

When testing the effect of reduction of I_{Ks}, the superfusate was switched to a buffer of the same composition as given above but containing antagonist Chromanol 293B (Sigma-Aldrich, St. Louis, MO). The final concentration of Chromanol 293B was 20 µM, consistent with the concentration used in previous study [40, 87]. At first, to increase I_{Ks}, agonist L364, 373 (3 µM, dissolved in DMSO) was used, however, once it became apparent that, at least at this concentration, it did not affect APDs, in subsequent experiments Mefenamic acid (100 µM, dissolved in 0.1M NaOH, Sigma-Aldrich, St. Louis, MO), was used as an agonist. Concentrations of L364, 373 and Mefenamic acid were the same as those used previously by Magyar et al. [45] for comparison with their results. After each drug was added, tissues were paced at 500 msec CL for 40 min for equilibration.

3.5 Data Analysis

The intracellular potentials were recorded using the commercial data acquisition system were analyzed offline using custom programs written in Matlab. Potentials were low pass filtered with a cutoff frequency of 1000 Hz, consistent with previous studies [15, 16, 21]. APDs were computed using two methods. For phase 1 and phase 2 of the study, a fixed threshold was determined by 90% of the amplitude of the action potential, and APD was defined as the duration between the points when the potential crossed the threshold during depolarization, i.e. start of an action potential and repolarization, i.e. end of an action potential. The threshold was determined using an action potential in the middle of each trial. For phase 3 of the study, APDs were calculated for each action potential as the

duration between the start of an AP, i.e. the point where the derivative of the potential becomes positive, and the instance when the cell repolarized to 90% of its amplitude. Although two different methods were used for APD calculation, in each study, random trials were selected and APDs were analyzed with both methods in those trials. Differences between APDs computed by the two methods were very small and the direction of difference was consistent, i.e. APDs computed by one method were consistently shorter or longer than those computed by the other method. Therefore, the method which we used to compute APD would not affect the results qualitatively.

From the restitution relationship between APD and DI obtained during the sinusoidal DI protocols (protocol 3.1-2, **Figure 3.7**), i.e. hysteresis loop as shown in **Figure 3.7**, five measures were computed to quantify memory, which are illustrated in **Figure 3.8** and described below: 1) loop thickness, referred as the difference in APDs between the ascending and descending phases when DI was at its mean value; 2) loop area, i.e. the area contained within the hysteresis loop; 3) overall tilt, defined as the slope of the line composed by connecting the two points where APDs were at its maximum and minimum; 4) maximum delay, which is the number of beats between the peaks of DI and APD; and 5) minimum delay, which is the delay (in number of beats) between the nadirs of DI and APD.

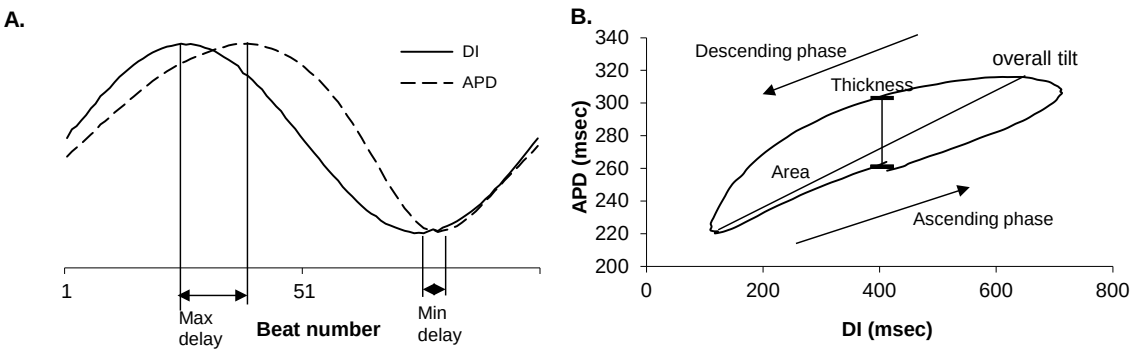

Figure 3.8 Illustration of measures for hysteresis loop.

A: The second cycle of oscillatory DIs (solid line) with 400 msec mean DI and the trace of resulting APDs (dashed line). To clearly show the measures of max delay and min delay, the trace of APDs is scaled and vertically offset to match the peak and nadir of the DI sequence (the maximal and minimal change in APDs was less than those in the DIs). Max delay and min delay are measured in beats. B: Hysteresis loop generated by the sequence of DIs in panel A, with illustration of loop thickness, overall tilt and loop area.

In some cases, APD adaptation caused baseline shift in the first cycle of the sinusoidal DI sequence, which was induced by the transition from 500 msec CL to constant DI pacing, therefore, we only computed the measures of hysteresis from the second cycle. In rare cases, DI control was transiently lost during real time control for 1 or 2 beats, in these cases the missed DI and corresponding APD values were replaced using linear interpolation from their adjacent 2 values. Those trials where DI control was lost for more than 5 beats in the 200 beats oscillatory DIs (2.5%) were excluded from further analysis. If there were more than one trial for any protocol that met the DI/CL control requirement stated above, then results from these trials were averaged and the measures were calculated from the averaged loop/restitution curve and used for further analysis.

For constant CL/DI protocols (protocol 4.1-2), alternans of APD was considered to occur when beat-to-beat difference in APDs (i.e. in long-short-long or short-long-short pattern) was $\geq$ 4 msec for at least 5 consecutive beats. The threshold of 4 msec is the same as that reported previously by Pruvot et al [33]. In the stepwise DI protocols (protocol 1.1-2, **Figure 3.4**), when alternans occurred, the following parameters were computed, which were then averaged: 1) the rate threshold of alternans onset and termination, i.e. the value of DI when alternans started, and the value of DI when alternans stopped; 2) the average amplitude of alternans (absolute value of the average difference between long and short APD) when DI was decreasing and when DI was increasing; 3) the average APD and the average CL at each level of DI.

3.6 Statistics

For phase 1 of the study, differences between the measures of onset and termination of alternans, or between the descending and ascending phase of DI were tested for statistical differences using a paired t-test. Significant difference was accepted at $p \leq 0.05$.

For phase 2, i.e. the heterogeneity study, as not all protocols could be completed in all four tissue samples from each animal, differences between endocardial and epicardial tissues and between the left and the right ventricular tissues were tested for statistical significance using a mixed model, which is a generalization of repeated measures ANOVA. Statistical analysis was conducted using SAS (SAS Institute Inc., NC). Significant difference was accepted at $p \leq 0.05$.

For the I_{Ks} study (phase 3), paired student t-test was conducted to test for statistical significance between all parameters during control and post-drug. Significant difference was also accepted at $p \leq 0.05$.

Chapter IV Results

4.1 Hysteresis in Threshold of APD alternans

As discussed in Chapter III, all analyses were conducted on data that were collected by the stand-alone acquisition system and processed off line. Therefore, the DIs computed off line differed slightly from the target DI for the control. We note that for the purposes of the current objective, it was not very important that a particular value of DI was met, rather, it was keeping DI invariant from one activation to next. DIs that were computed off-line and are reported in the results section were the actual DIs experienced by the myocyte from which TMPs were obtained. As **Figure 4.1A** shows, due to conduction delays, the resulting DIs were slightly different than the target DIs (dashed line, which is also shown in **Figure 3.4**). However, the figure also shows that the important criterion of minimizing beat by beat changes in DI was met.

In the 30 beats stepwise DI protocol (protocol 1.1, **Figure 3.4**), alternans was observed in 4 out of the 6 pigs. This incidence of APD alternans is consistent with results of previous studies in pigs [9]. The averaged trace of APDs is shown in **Figure 4.1B**. In the other 2 pigs, decrease of DI led to 2:1 block, with no transition to 2:2 rhythm, i.e. alternans. In all trials when alternans occurred, hysteresis between the onset and termination of alternans was observed, transition from 2:2 rhythm, i.e. alternans of APD, back to 1:1 rhythm occurred at longer DI than the transition from 1:1 to 2:2 rhythm, i.e. initiation of alternans. **Figure 4.2A** shows the DI values for onset and termination of APD alternans in each animal where alternans was observed.

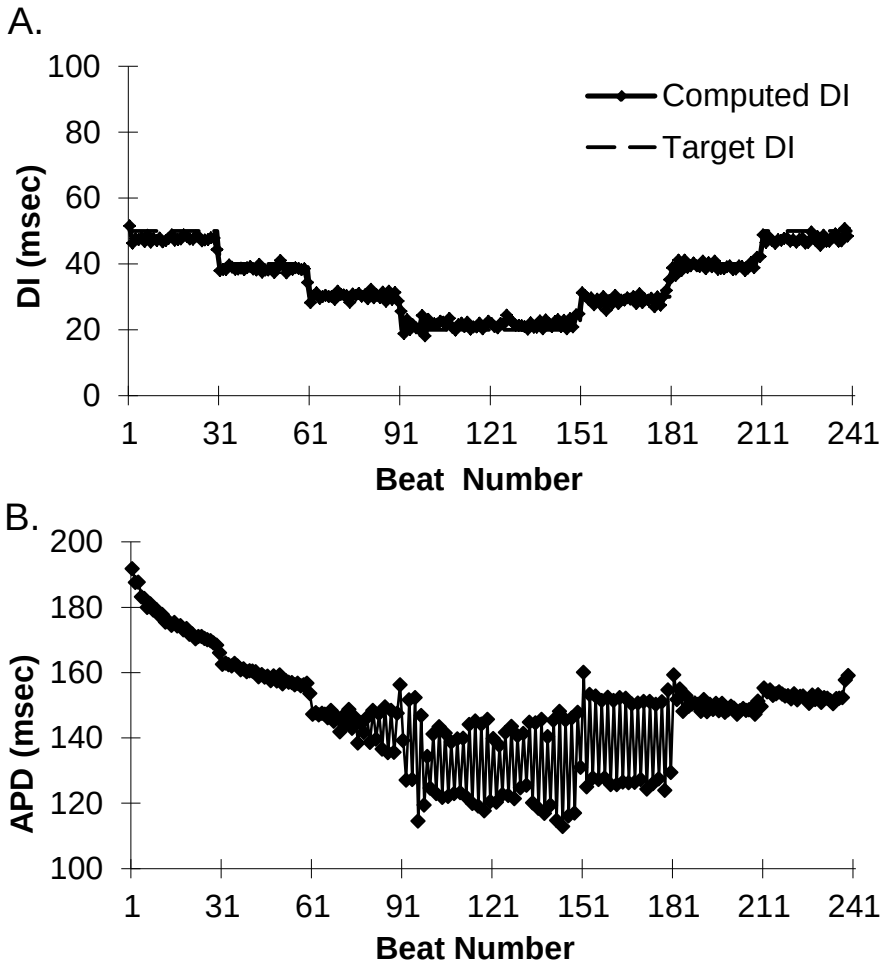

Figure 4.1 Average step DI sequence and the resulting APDs for the 30 beats stepwise DI protocol.

A: Overlay of the target DI sequence with DIs calculated from offline analysis. B: The averaged trace of APD resulting from the computed DI sequence shown in A.

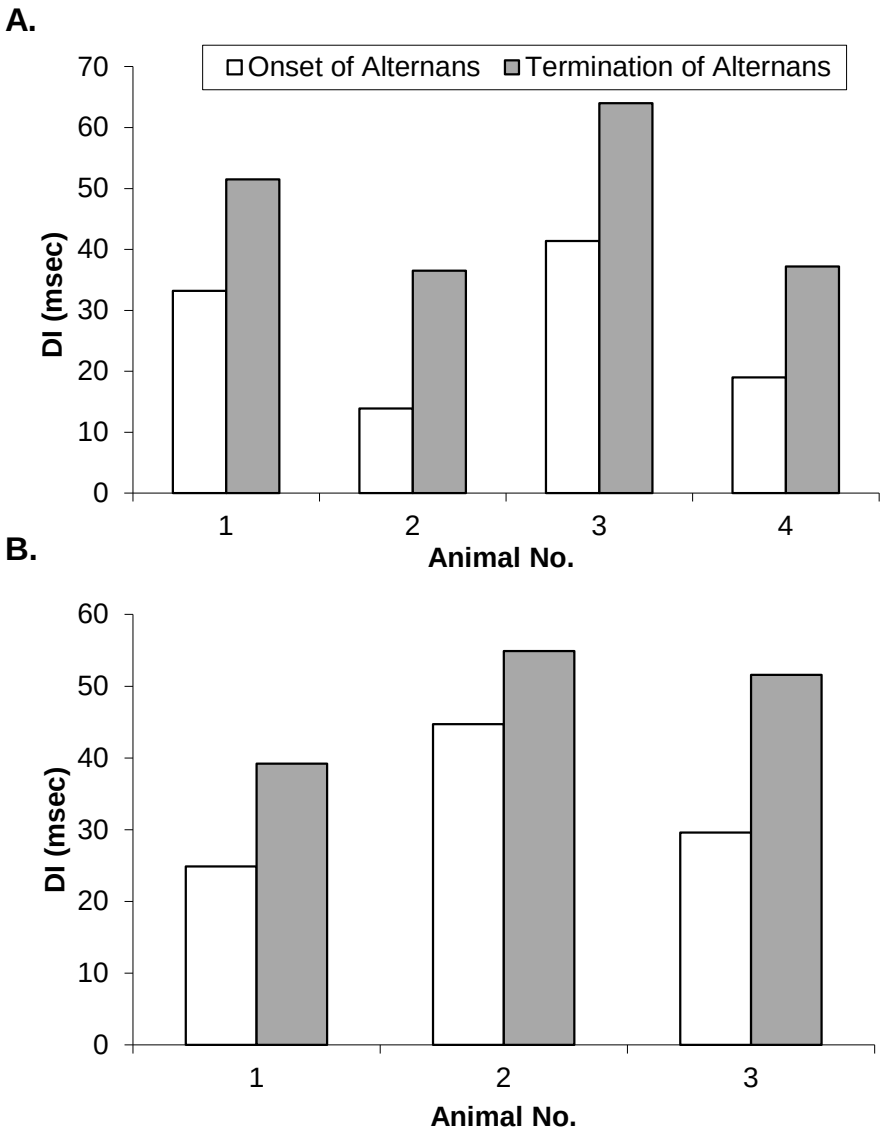

Figure 4.2 DI values for onset and termination of alternans in each animal during 30 beats (A) and 15 beats (B) stepwise DI protocols.

Figure 4.3 shows an example of the hysteresis of alternans from one trial. The figure shows that alternans occurred at DI equal to 34 msec during the DI descending phase, and persisted until DI increased to 53 msec. On average, alternans started at 27±6 msec DI during the descending phase and persisted until 47±6 msec DI during the ascending phase. The CLs corresponding to these thresholds were 162±32 msec and 182±32 msec (both changes had $p<0.05$).

Figure 4.4 shows a plot of averaged APD alternans amplitude for the 30 beats stepwise DI protocol. The figure shows that at the same level of DI, the average amplitude of alternans was greater during DI ascending phase than the DI descending phase. The average amplitude of alternans was 22±9 msec when DIs were decreasing, and was 26±11 msec when DIs were increasing. The average area of the hysteresis loop was 197 $msec^2$. A summary of these results is shown in **Table 4.1**.

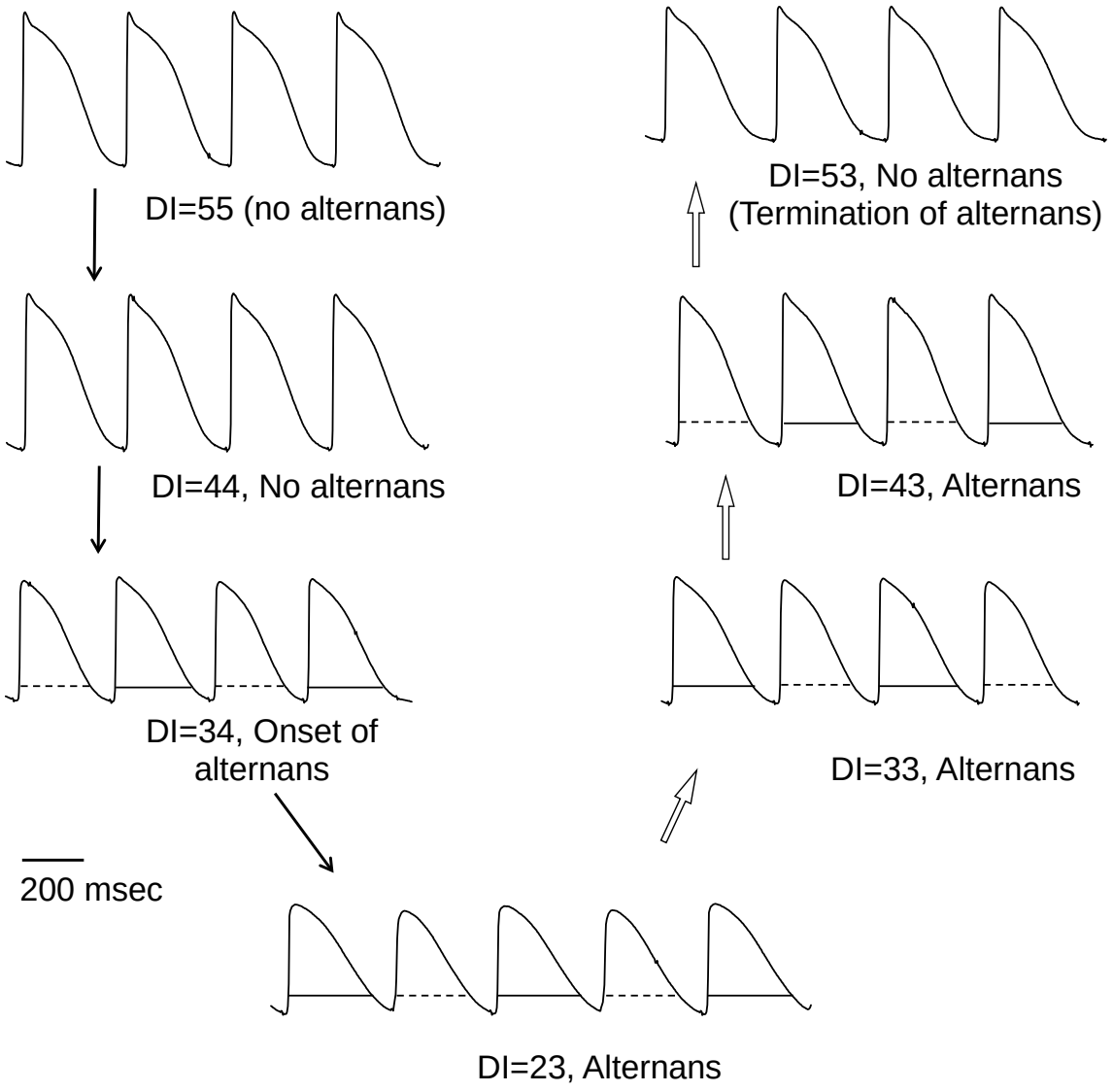

Figure 4.3 Example of TMPs from endocardial tissue showing hysteresis in the state transition.

The figure shows that during the descending phase of DI (black arrows), the transition from 1:1 rhythm to 2:2 (alternans) rhythm, i.e. onset of alternans, occurred at DI = 34 msec, with an amplitude of 5~6 msec. The APD alternans persisted at DI = 23 msec, with an increased amplitude of about 25 msec. During DI ascending phase (white arrows),

alternans of APD persisted at DI = 33 and 43 msec with decreased amplitudes of 8~9 msec and 5~6 msec respectively, and terminated (transition back to 1:1 rhythm) at DI = 53 msec. Solid and dashed lines on the AP traces represent long and short APDs, respectively.

Table 4.1 Summary of Hysteresis Results for Stepwise DI Protocols

Beats at each Level of DI	**DI (msec)**		**CL (msec)**		**Average Alternans Amplitude (msec)**	
	Onset	***Termination***	***Onset***	***Termination***	***DI Decrease***	***DI Increase***
30 (N=4)	27±6*	47±6*	162±32‡	182±32‡	22±9	26±11
15 (N=3)	33±6†	49±5†	175±37	194±38	13±3	15±4

Onset (termination) DI/CL for alternans: the value of DI/CL (Mean±SEM, in milliseconds) when alternans of APD started (terminated). The table shows that in both protocols, APD alternans terminated at longer DIs and CLs than the initiation. */‡ indicate significant differences between the onset and termination DI/CL in the 30 beats protocol; † indicates significant difference between the onset of termination DI in the 15 beats protocol.)

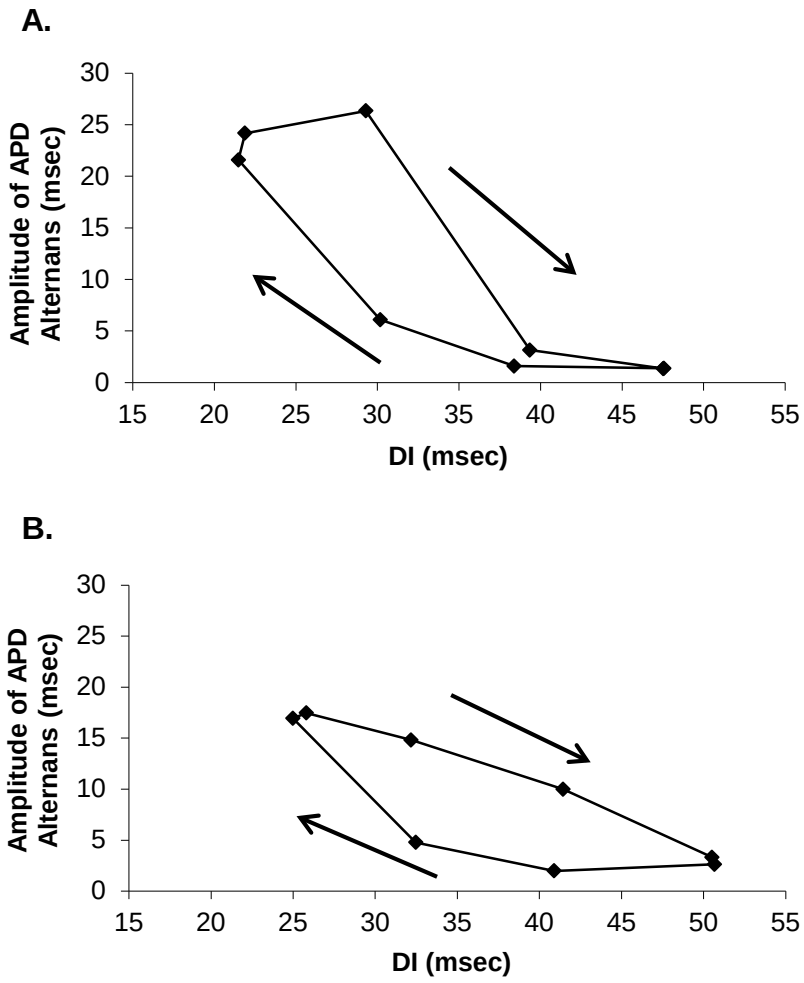

Figure 4.4 Averaged amplitude of alternans of APD for 30 beats (A) and 15 beats (B) stepwise DI protocols.

Each black dot represents mean amplitude of APD alternation at that level of DI. Arrows refer to directions of changes in DI. The figure indicates that at the same level of DI, the amplitude of APD alternans was larger at DI ascending phase than DI descending phase during both protocols.

During the 15 beats stepwise DI protocol (protocol 1.2, **Figure 3.4**), alternans occurred in 3 out of 6 pigs. Similar to the 30 beats stepwise protocol, hysteresis was consistently observed whenever alternans occurred. **Figure 4.5** shows the averaged DI trace and the averaged APD trace. Overall, the difference between onset and termination threshold for alternans was smaller than the 30 beats stepwise protocol, and significant difference was obtained only between the DIs at the initiation and termination of alternans. On average, alternans started at 33±6 msec DI (175±37 msec CL) and stopped at 49±5 msec DI (194±38 msec CL). The DI values where onset and termination of APD alternans occurred in each animal are shown in **Figure 4.2**. Same as during the 30 beats stepwise protocol, **Figure 4.4B** shows an averaged hysteresis plot during 15 beats stepwise protocol. The alternans amplitude, although generally smaller than that during the 30 beats stepwise protocol, was still larger during DI ascending phase compared to descending DIs. The average amplitude of alternans was 13±3 msec when DIs were decreasing, and was 15±4 msec when DIs were increasing. Compared to the 30 beats stepwise protocol, the loop area was smaller (160 $msec^2$). These results are summarized in **Table 4.1**.

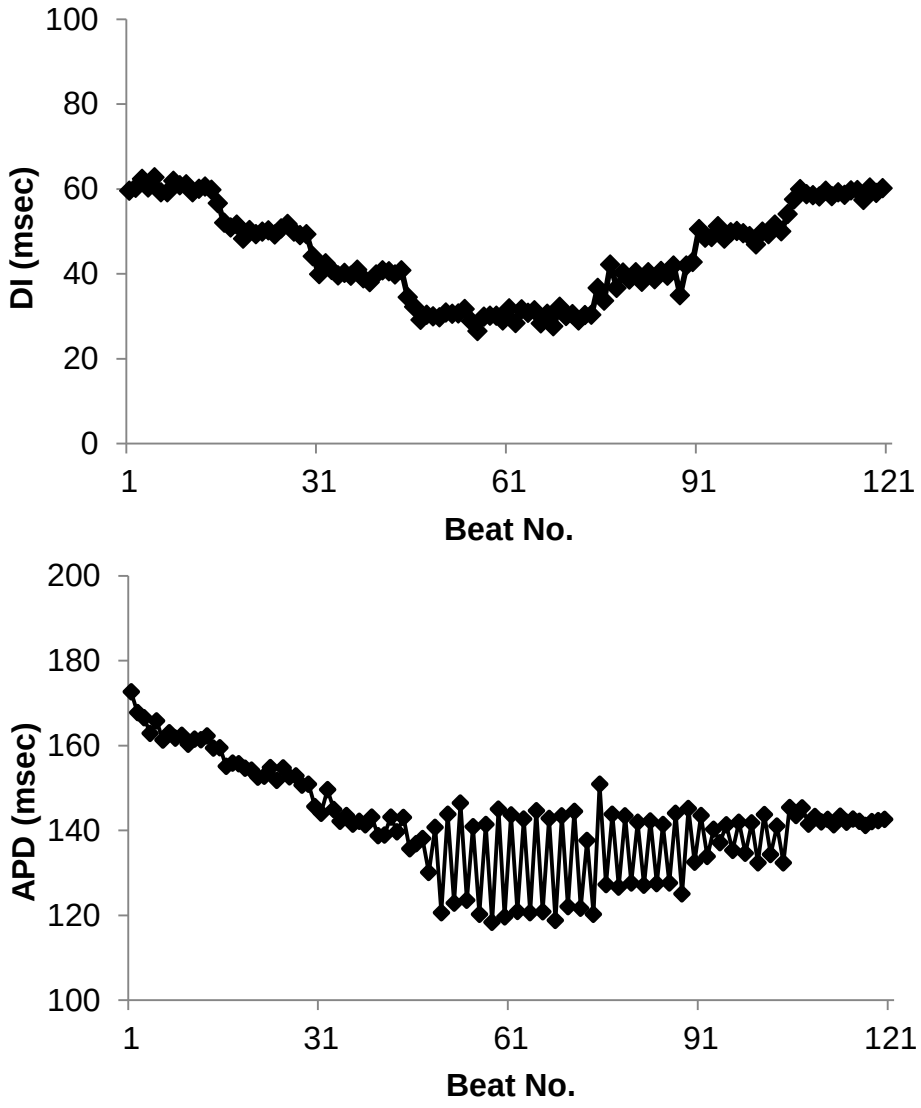

Figure 4.5 Stepwise DI protocol with 15 beats in each step (A) and the averaged trace of APD (B) resulting from the DI sequence shown in A.

4.2 Heterogeneous Action Potential Duration

Panels A-D in **Figure 4.6** show an example of TMPs recorded from right and left ventricular endocardium and epicardium. Panel E shows an overlay of the TMPs, with the start of action potentials aligned, shown in panels A-D to clearly depict differences among the action potentials. **Figure 4.6** shows that, consistent with previous studies in pigs and other species [88, 89], APDs from the epicardium, either the left or the right, were shorter than those from endocardium. These differences in mean APDs computed during 500 msec constant CL pacing were 251±11 vs. 186±9 msec for right ventricular endocardium (N=9) and epicardium (N=8, $p<0.01$), and 231±10 vs. 174±8 msec for left ventricular endocardium (N=9) and epicardium (N=10, $p<0.01$). For myocytes from the same layer, i.e. endocardium or epicardium, the difference in mean APDs was 20 and 12 msec between the two ventricles, but this difference was not statistically significant.

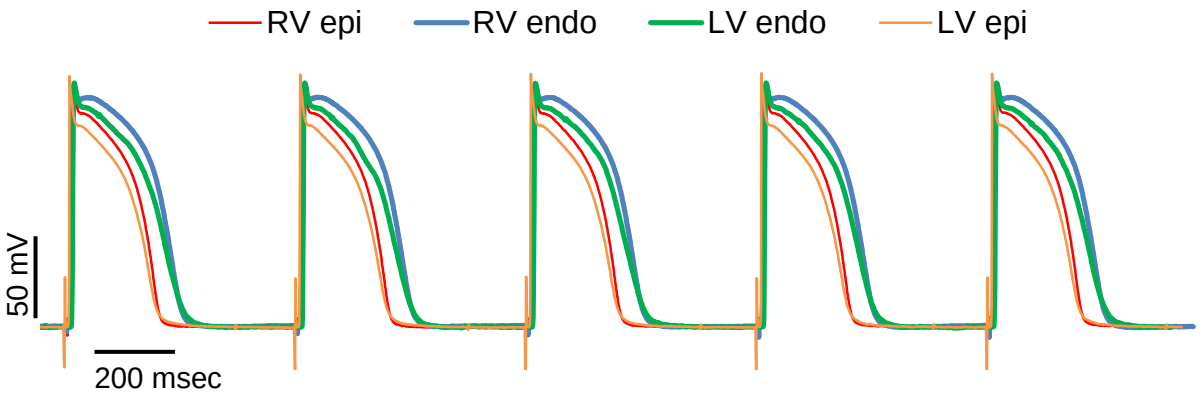

Figure 4.6 Examples of transmembrane action potentials (TMPs) recorded from 4 types of myocytes from four different tissues.

4.3 Heterogeneity in Restitution

Figure 4.7 shows average restitution curves obtained using the standard (protocol 2.1, **Figure 3.5**) and the dynamic (protocol 2.2, **Figure 3.6**) protocols in two tissue samples. The right and left ventricular epicardial restitution curves were obtained in tissues from same animals, while the endocardial restitutions were obtained in tissues from different animals. In order to obtain a measure of slope over the entire range of DIs spanned by restitution assessment, the instantaneous slopes were calculated between each successive APD and DI pairs and then averaged for all values of DI to obtain an overall slope. The overall slopes are shown in **Table 4.2**. One should note that although the overall slopes are generally smaller than one, at shorter CL, there was at least one instantaneous slope greater than one for all dynamic restitution curves and endocardial standard restitution curves.

Table 4.2 Overall Restitution Slopes in Different Tissue Types

	RV Endo	RV Epi	LV Endo	LV Epi
Standard	0.56	0.34	0.53	0.22
Dynamic	1.03	0.56	0.93	0.53

Average of restitution slopes from two tissue samples each. Instantaneous slopes of restitution functions were averaged over all values of DI to obtain an overall slope. RV: right ventricle; LV: left ventricle; endo: endocardium; epi: epicardium.

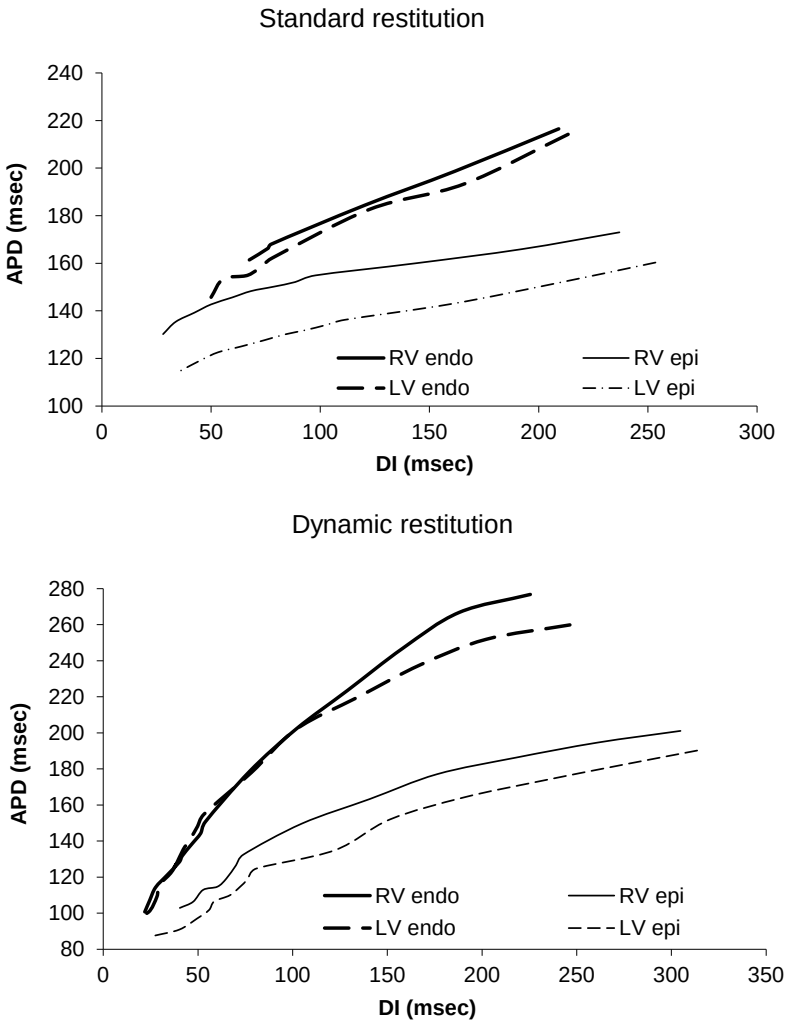

Figure 4.7 Averaged standard and dynamic restitution curves obtained from tissues (N=2) from the endocardium and the epicardium of left and right ventricles.

4.4 Heterogeneity in Memory

Figure 4.8 shows the average relationships of APD vs DI with error bars equal to the standard errors of mean (SEM) obtained from 400 msec sinusoidal DI protocol (protocol 3.1, **Figure 3.7**). The hysteresis loops obtained during multiple trials were averaged within each tissue type within an animal and then averaged across animals. The error bars in **Figure 4.8** to some extent overestimate the degree of variation in the hysteresis loops across animals used in our experiments as they are largely influenced by the differences in baseline APDs among different pigs. Thus the error bars do not accurately represent the variation in the degree of hysteresis in restitution. The restitution relationships without error bars are shown in **Figure 4.9**. For the ease of comparison between tissue types, we superimposed hysteresis loops in each panel by vertically offsetting the loops to account for differences in baseline APDs. Measures of memory were consistently larger in the right ventricular endocardium than those in the epicardium: loop thickness (34.5±2.3 msec vs. 24.7±2.3 msec, $p < 0.05$), overall tilt (0.185±0.013 vs. 0.102±0.006, $p < 0.05$) and loop area (16154±980 $msec^2$ vs. 11599±1006 $msec^2$, $p < 0.05$). Although we found similar trends in these parameters between the endocardium and the epicardium in the left ventricle, only differences in overall tilt were statistically significant (**Figure 4.9B**, 0.141±0.011 vs. 0.102±0.014 msec, $p < 0.05$). There were no statistically significant differences in these measures between the two ventricles for both the endocardial and the epicardial tissues except for two: the overall tilt in the endocardial tissues from the right ventricle was larger than that in the endocardial tissues from the left ventricle (**Figure 4.9C**, 0.185±0.013 vs. 0.141±0.011 msec, $p < 0.05$) and the min delay from the epicardial tissues in the left ventricle was larger than that in the epicardial tissues from the right

ventricle (**Figure 4.9D**, 3.3±0.8 vs. 1.6±0.4 beats, p=0.05). A summary of these measures (mean ± SEM) is provided in **Table 4.3**.

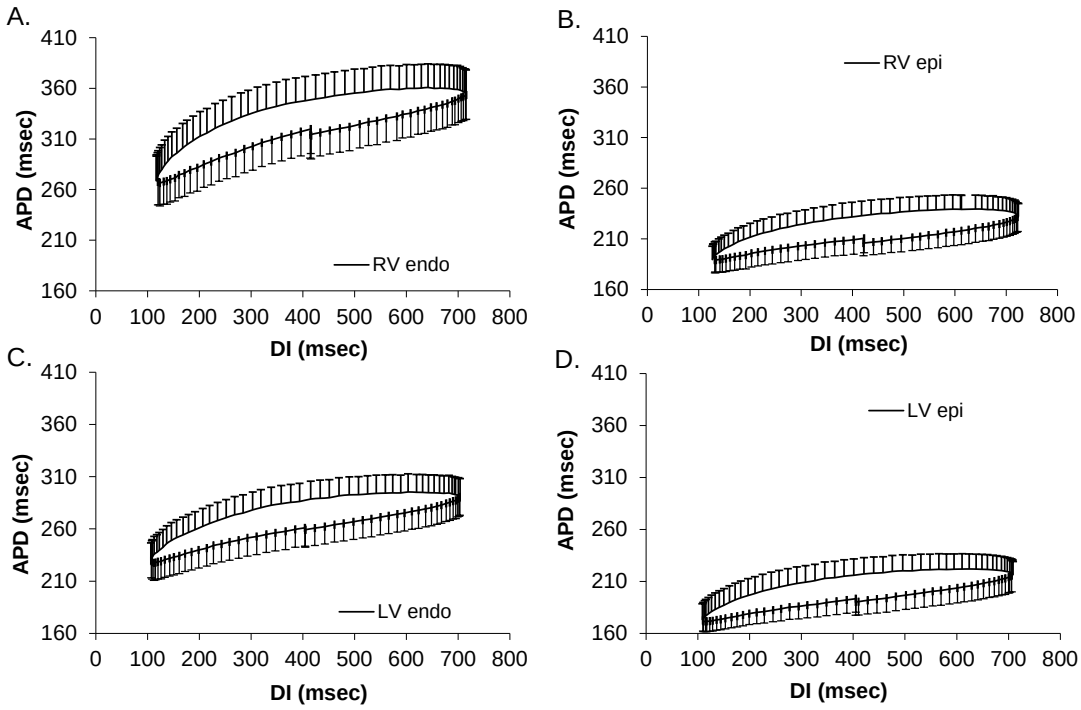

Figure 4.8 Averaged (N=8) hysteresis loop with error bars (± SEM) resulted by sinusoidal DI trial with mean DI = 400 msec (protocol 3.1).

A: RV endocardium, B: RV epicardium, C: LV endocardium, D: LV epicardium

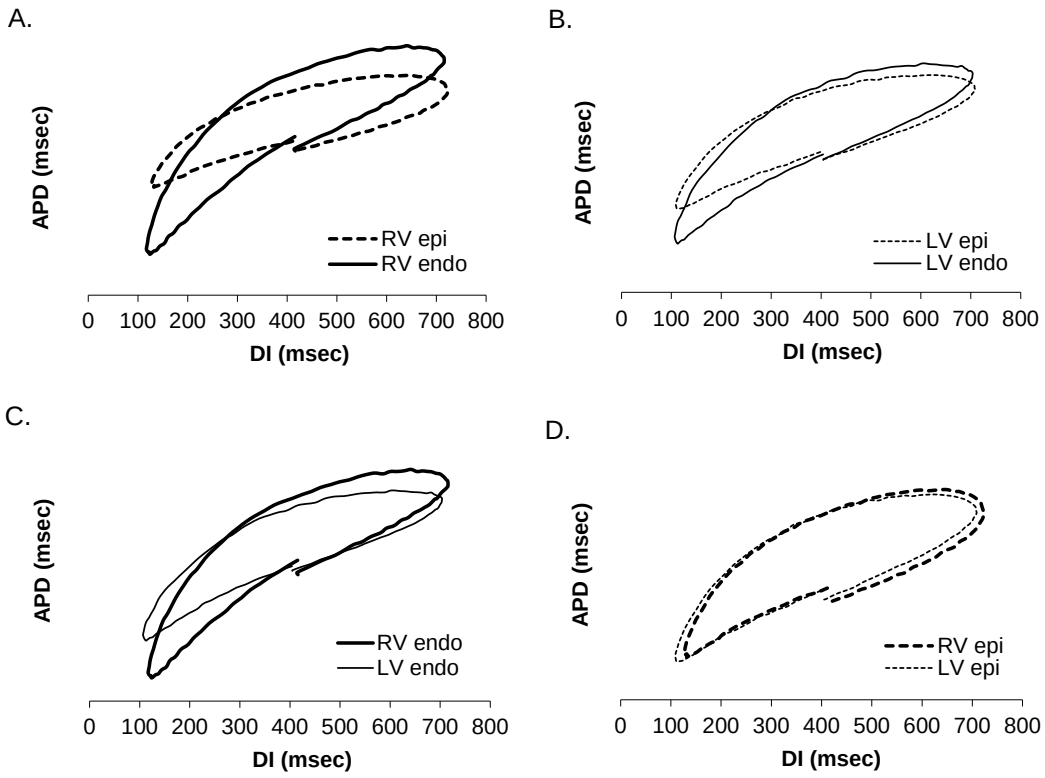

Figure 4.9 Averaged restitution relationship of APDs during sinusoidal DI sequence with mean DI = 400 msec (protocol 3.1).

A: RV endocardium (N=8) vs. RV epicardium (N=8). The loop thickness, overall tilt and area were significantly different between the two loops. B: LV endocardium (N=8) vs. LV epicardium (N=8). Only the overall tilt was significantly different between the two loops. C: RV endocardium (N=8) vs. LV endocardium (N=8). As in panel B, only overall tilt was significantly different between the loops. D: RV epicardium (N=8) vs. LV epicardium (N=8). Only the min delay was significantly different between the loops. The loops have been offset vertically to facilitate comparison in the figures, however, these offsets were used only in making these figures and were not used in computation of measures of memory.

Table 4.3 Summary of measures of memory for the 400 msec DI sequence

	RV endo (N=8)	RV epi (N=8)	LV endo (N=8)	LV epi (N=8)
Thickness (msec)	34.5±2.3*	24.7±2.3*	29.2±2.6	24.9±2.7
Overall tilt	0.185±0.013*#	0.102±0.006*	0.141±0.011Δ#	0.102±0.014Δ
Area (msec^2)	16154±980*	11599±1006*	13040±1452	11731±1453
Max delay (beats)	11±1.2	12±0.74	13±1.3	13±0.44
Min delay (beats)	2.5±0.6	1.6±0.4◊	3.1±0.5	3.3±0.8◊

A summary of mean (±SEM) values of measures of hysteresis for 400 msec DI sequence. * indicates significant ($p \leq 0.05$) difference between RV endo and RV epi; # indicates significant difference between RV endo and LV endo; Δ indicates significant difference between LV endo and LV epi; ◊ indicates significant difference between LV epi and RV epi.

As discussed above, the variations were overestimated because of the variation in baseline APDs across animals. To minimize this problem, the hysteresis in restitution was normalized within each pig such that the maximum and minimum change in APD was between +1 and -1. The normalized hysteresis loops were then averaged across all pigs. These averages with the normalized standard errors of mean for the 150 msec sinusoidal DI protocol (protocol 3.2, **Figure 3.7**) are shown in **Figure 4.10**. **Figure 4.10** shows that the hysteresis loops were highly consistent across animals for all types of myocytes. The maximum standard errors for the normalized APDs were ±0.09 (4.5%) for the 150 msec sinusoidal DI protocol. **Figure 4.11**, drawn in the same format as **Figure 4.9**, shows hysteresis in restitution observed during the 150 msec sine DI protocol. The degree of heterogeneity in hysteresis within ventricles, i.e. between endocardium and epicardium from the same ventricle, was generally larger than that observed during the 400 msec sine DI protocol. Significant differences ($p < 0.05$) were observed in the measures of thickness, overall tilt and loop area between endocardium and epicardium, in both left and right ventricles (**Table 4.4**). Percentage differences between endo- and epicardium in loop thickness, loop area and overall tilt were 40%, 43% and 34% for the right ventricle and 40%, 29% and 38% for the left ventricle. Similar to the 400 msec sine DI protocol, no significant differences were observed between the two ventricles for the 150 msec sine DI protocol, although the measures of thickness and areas tended to be larger in the right ventricular endocardium than the left ventricular endocardium for both protocols.

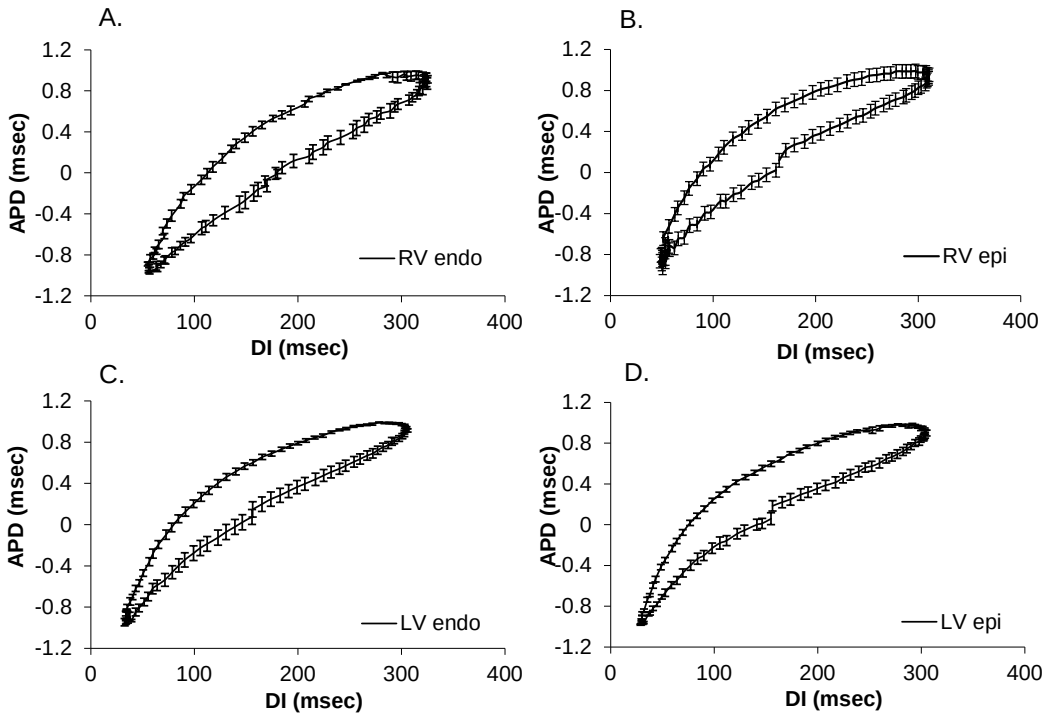

Figure 4.10 Normalized average hysteresis loop with error bars (± SEM) resulted by sinusoidal DI trial with mean DI = 150 msec.

A: RV endocardium (N=7), B: RV epicardium (N=5), C: LV endocardium (N=7), D: LV epicardium (N=7).

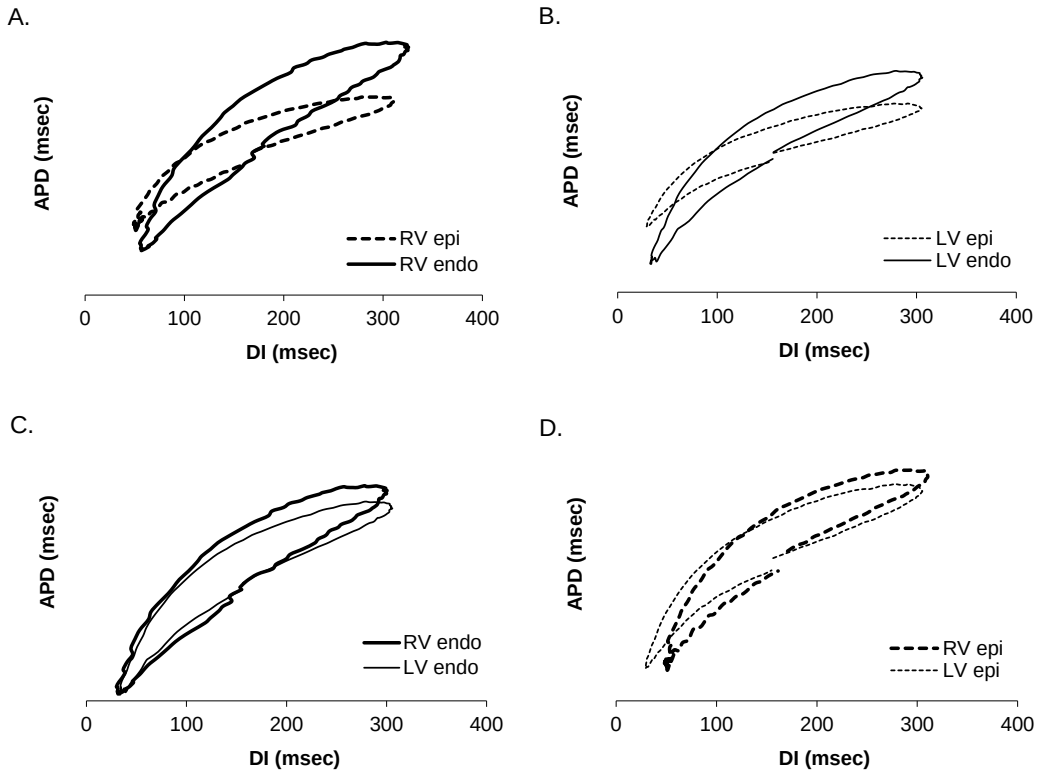

Figure 4.11 Averaged restitution relationship of APDs during sinusoidal DI sequence with mean DI = 150 msec (protocol 3.2).

A: RV endocardium (N=7) vs. RV epicardium (N=5). The loop thickness, overall tilt and area were significantly different between the two loops. B: LV endocardium (N=7) vs. LV epicardium (N=7). The loop thickness, overall tilt and area were significantly different between the two loops. C: RV endocardium (N=7) vs. LV endocardium (N=7). No significant differences between the loops were observed. D: RV epicardium (N=5) vs. LV epicardium (N=7). No significant differences between the loops were observed. As in **Figure 4.9**, the loops have been offset vertically to facilitate comparison, however, these offsets were used only in making these figures and were not used in computation of measures of memory.

Table 4.4 Summary of measures of memory for 150 msec DI sequence

	RV endo (N=7)	RV epi (N=5)	LV endo (N=7)	LV epi (N=7)
Thickness(msec)	26.9±3.7*	16.2±1.0*	22.3±2.1Δ	13.3±2.2Δ
Overall tilt	0.376±0.054*	0.249±0.015*	0.351±0.031Δ	0.219±0.025Δ
Area(msec2)	7288±899*	4146±523*	6443±488Δ	4559±470Δ
Max delay(beats)	9.9±1.6	7.4±1.5	9.4±0.9	7.4±1.3
Min delay(beats)	3.3±1.0	3.6±1.2	1.7±0.6	2±0.6

A summary of mean (±SEM) values of measures of hysteresis for 150 msec DI sequence * indicates significant ($p < 0.05$) difference between RV endo and RV epi; Δ indicates significant difference between LV endo and LV epi.

4.5 Alternans in DI Dependent and Independent Mechanisms

Results from our previous studies showed that alternans of APD have both DI dependent and independent mechanisms in canine right ventricular endocardial tissues. In order to test whether DI independent alternans is present in both left and right endocardial and epicardial tissues in pigs, we used constant CL/DI protocols (protocol 4.1-4.2) to investigate APD alternans. APD alternans was observed in 3 pigs during constant DI pacing and in 4 pigs alternans occurred during constant CL pacing, in both endocardium and epicardium of the two ventricles. Examples of alternans of APD recorded during constant CL pacing (CL = 110 msec) and constant DI pacing (DI = 25 msec) is shown in **Figure 4.12**. The trial with constant CL pacing recorded from right ventricular endocardium shows alternating APDs accompanied by alternating DIs, while the trial recorded from left ventricular epicardium during constant DI pacing shows alternating APDs with minimal changes in DIs and thus, alternating CLs. For all beats where alternans was observed, instantaneous slopes between successive pairs of APDs and DIs were calculated. A histogram of the instantaneous slopes during constant CL and DI pacing is shown in **Figure 4.13**. Consistent with previous studies in canines [17], the slope during constant CL was always equal to 1, while during constant DI pacing, since the changes in DI were minimal (< 4 msec) compared to the changes in APD (> 4 msec), slopes were more uniformly distributed and mostly greater than 1. As shown in the figure, most slopes fall into the +/- 10 group. Also, unlike constant CL pacing, slopes during constant DI pacing could be negative, i.e. APD increased while the preceding DI decreased.

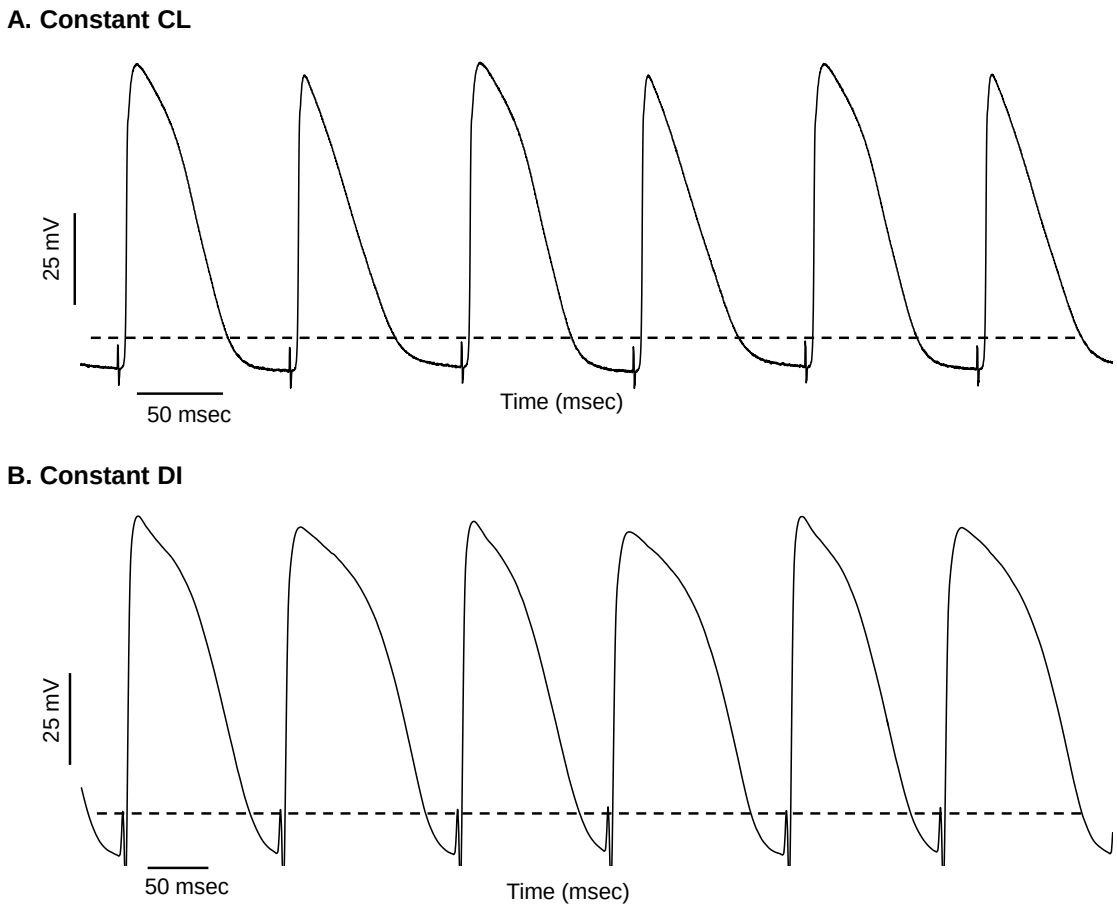

Figure 4.12 Examples of APD Alternans during Constant CL Pacing and Constant DI Pacing.

A: TMPs recorded in right ventricular endocardium showing APD alternans during constant CL pacing, CL = 110 msec. B: TMPs recorded in left ventricular epicardium showing APD alternans during constant DI pacing, DI = 25 msec.

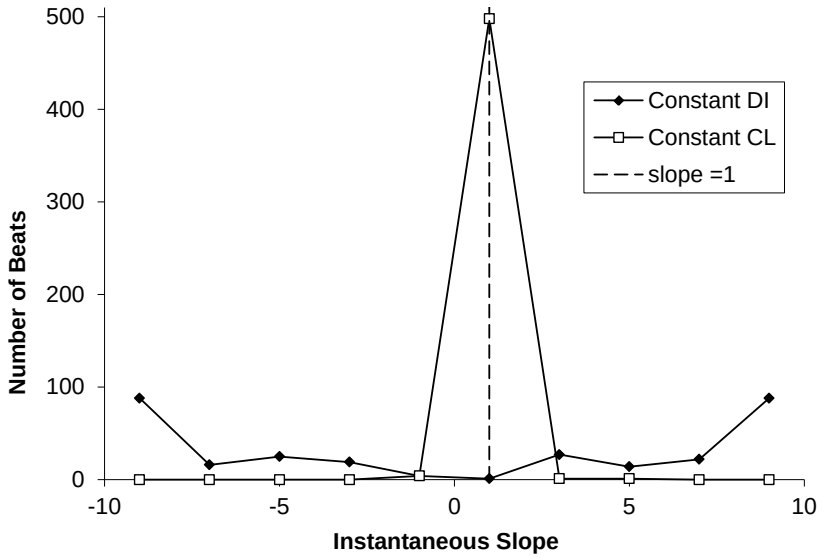

Figure 4.13 Instantaneous slopes during alternans observed in constant CL pacing and constant DI pacing.

4.6 Effects of I_{Ks} Change on Baseline APDs

Because L364, 373 had been reported as a selective I_{Ks} agonist in previous studies of guinea pigs [90] and rabbits [91], we tested the effect of L364, 373 on pig ventricular APDs in the first animal. However, APDs at 500 msec CL showed no difference between control and post drug (227 msec vs 222 msec). This observation, i.e. lack of an effect of this drug, is consistent with a previous study in dogs [45]. As the main objective of the current study was to explore the effect of changes in I_{Ks} on dynamics of repolarization of AP, and not the effect of L364, 373, for the rest experiments we used a relatively non-selective agonist, Mefenamic acid, to activate I_{Ks}.

Figure 4.14 shows an example of TMPs recorded at 500 msec constant CL pacing before (solid line) and after application of I_{Ks} antagonist Chromanol 293B (dashed line) and agonist Mefenamic acid (dotted line). All the traces were collected from one animal and the upstroke of APs were aligned to better show the difference among APDs. The average APD (N=6) was lengthened by 14% after Chromanol 293B (205.5±6.3 msec vs 234.6±7.3 msec); after Mefenamic acid, the average APD (N=6) was shortened by 20%, i.e. from 218.6±4.5 msec to 173.7±6.2 msec. Both changes were significant.

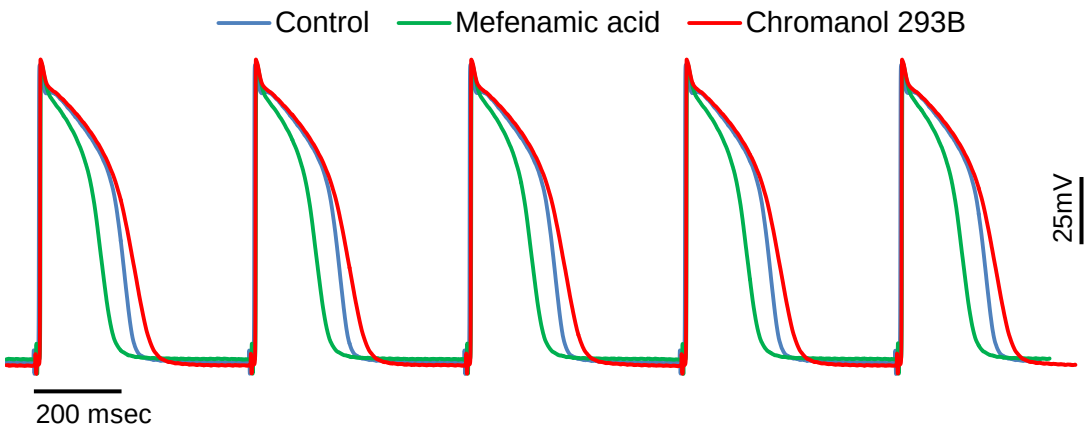

Figure 4.14 Example of TMPs at CL of 500 msec during control and post-drug.

The figure shows TMPs recorded in one pig with APD differences among control (solid line), Chromanol 293B (dashed line) and Mefenamic acid (dotted line) data. APD increased after Chromanol 293B and decreased after Mefenamic acid.

4.7 Effects of I_{Ks} Change on Restitution

To quantify changes in restitution, standard and dynamic restitution (protocol 2.1 and 2.2) were obtained from all animals. **Figure 4.15** shows examples of standard and dynamic restitution during control and post-drug in one animal. For each restitution curve, overall slope was obtained by computing the average value of all slopes over the entire range of DIs. Average overall slopes (N=6) are summarized in **Table 4.5**. Compared to control, both standard (**Figure 4.15A**) and dynamic restitution (**Figure 4.15B**) had steeper slopes after Chromanol 293B, especially at short CL, however, only the slopes of dynamic restitution were significantly different (0.75 control vs. 0.97 Chromanol 293B). In contrast, slopes of both standard and dynamic restitution flattened after Mefenamic acid (**Figure 4.15C** and **D**), both were significantly smaller than the control (0.26 vs. 0.45 for standard, and 0.59 vs. 0.91 for dynamic). In general, for both drugs, changes in slope of dynamic restitution were more prominent than that of standard restitution. Average slopes for each restitution curve were also computed for all points where CL < 300 msec, as alternans was mostly observed in this range of CL in previous studies. These results are shown in **Table 4.5**. As shown in the table, all slopes were larger at shorter CL compared to the overall slopes, and all dynamic slopes were close to or greater than 1, a condition believed to be requisite for occurrence of alternans and decrease in electrical stability.

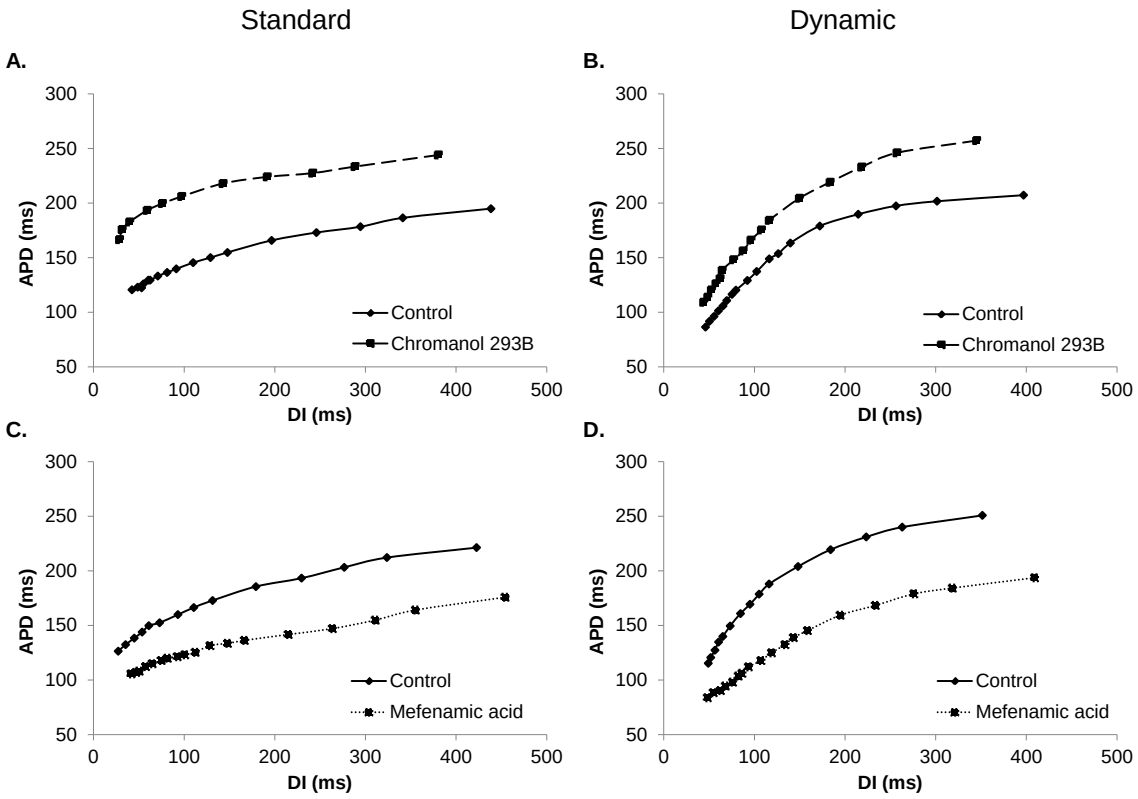

Figure 4.15 Standard (A and C) and dynamic (B and D) restitution curves during control and post-drugs.

The restitution curves were recorded from one trial and show the change in slope of restitution with application of Chromanol 293B (A and B) and Mefenamic acid (C and D). Slopes in this trial are comparable to the average slopes over all experiments (N=6). Slopes of standard and dynamic restitution both increased after Chromanol 293B and decreased after Mefenamic acid, but the changes were more prominent in dynamic restitution.

Table 4.5 Average (N=6) Overall Slopes for Standard and Dynamic Restitution during control and post-drugs.

		Control	Chromanol 293B	Control	Mefenamic acid
Standard	Overall	0.30±0.05	0.44±0.09	0.45±0.08	0.26±0.03*
	CL≤300	0.45±0.06	0.67±0.15	0.63±0.13	0.34±0.04*
Dynamic	Overall	0.75±0.12	0.97±0.15*	0.91±0.11	0.59±0.08*
	CL≤300	1.08±0.14	1.29±0.23	1.19±0.15	0.81±0.09*

Slopes at all values of DIs in each restitution curve were averaged to obtain an overall slope, and slopes at values of DIs with CL ≤ 300 msec were averaged to obtain the slope for short CL. *: $p<0.05$.

4.8 Effects of I_{Ks} Change on Memory

Hysteresis in restitution, i.e. memory, was observed in both sinusoidal DI protocols (protocol 3.1-2, **Figure 3.7**). **Figure 4.16** shows the averaged hysteresis loops (N=5, due to technical difficulties with DI control, we could not obtain data during the 400 msec DI protocol in one animal) for the 400 sine DI protocol (protocol 3.1, **Figure 3.7**). In the 5 measures of hysteresis, most prominent change was observed in loop thickness and area: after Chromanol 293B (**Figure 4.16A**), loop thickness increased from 13.2±2.2 msec to 16.7±2.4 msec and area enlarged from 8083.7±1303.2 $msec^2$ to 11191±1874.8 $msec^2$, the percentage change was 26.5% and 27.8%, respectively; oppositely, with Mefenamic acid (**Figure 4.16B**), loop thickness decreased from 15.7±1.7 msec to 7.6±1.1 msec, and area shrank from 8960.1±664.4 $msec^2$ to 4214.5±810.3 $msec^2$, the percentage change was 51.9% and 53% (all changes significant). Overall tilt showed inconsistent changes during both

drugs across animals, where both increases and decreases were observed, resulting in minimal average change between control and post-drug. Changes in max and min delay were also minimal and no significant differences were present. **Table 4.6** includes a summary of these measures (mean±SEM) for 400 msec sine DI protocol.

Table 4.6 A summary of mean (±SEM) values of measures of hysteresis for 400 msec DI protocol for both drugs (control and post-drug), N=5.

	Control	Chromanol 293B	Control	Mefenamic acid
Thickness (msec)	13.2±2.2	16.7±2.4*	15.7±1.7	7.6±1.1*
Overall Tilt	0.065±0.017	0.070±0.023	0.080±0.017	0.063±0.015
Area ($msec^2$)	8083.7±1303.2	11191±1874.8*	8960.1±664.4	4214.5±810.3*
Max delay (beats)	20.0±2.5	23.4±2.1	17.6±3.1	17.2±0.9
Min delay (beats)	1.2±0.2	2.6±0.7	2±0.5	3.2±0.9

***: $p < 0.05$**

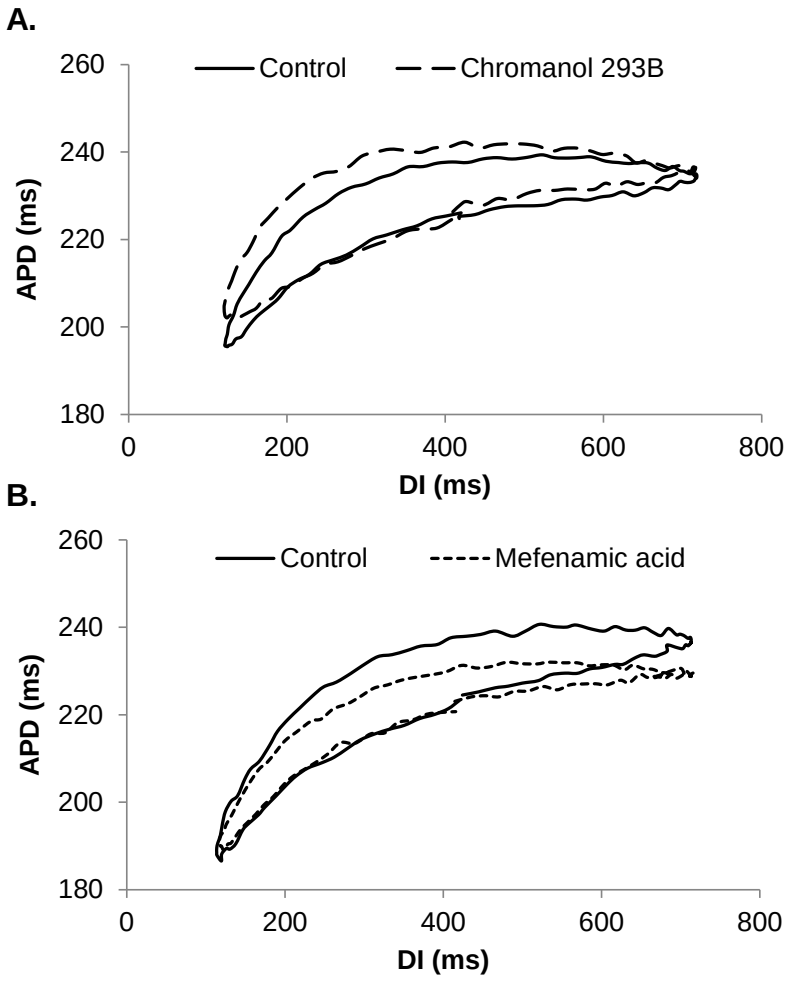

Figure 4.16 Averaged restitution relationship (N=5) of APD vs. DI during 400 msec sinusoidal DI protocol (protocol 3.1) for control and post-drug.

A: Control (solid line) vs. Chromanol 293B (dashed line), loop thickness and area increased significantly after Chromanol 293B. B: Control (solid line) vs. Mefenamic acid (dotted line), significant decrease in loop thickness and area were observed after Mefenamic acid. Curves with drug manipulation were shifted vertically (to adjust for differences in APD) in both panels to facilitate comparison between the hysteresis loops. Labels of the vertical axis represent the APD values of the control curve.

Figure 4.17 shows the averaged hysteresis loops (N=6) of control and post-drug data obtained from the 150 msec sinusoidal DI protocol (protocol 3.2, **Figure 3.7**). The results are similar to that during the 400 msec sine DI protocol; loop thickness and area were significantly different while the changes in overall tilt were mixed. In percentage, loop thickness increased 51.6% after Chromanol 293B and decreased 29.2% after Mefenamic acid, and the change in area was 31.4% increase and 35.3% decrease, respectively. A summary of these measures is in **Table 4.7**.

Table 4.7 A summary of mean (±SEM) values of measures of hysteresis for 150 msec DI protocol, N=6.

	Control	Chromanol 293B	Control	Mefenamic acid
Thickness (msec)	15.3±2.3	23.2±2.3*	19.2±1.1	13.6±1.8*
Overall Tilt	0.257±0.035	0.234±0.028	0.311±0.039	0.259±0.045
Area (msec2)	4282.5±635.6	5629.2±954.4*	5267.3±745.1	3409.1±534.7*
Max delay (beats)	9.6±1.5	10.2±1.1	7.6±1.3	5.7±1.4
Min delay (beats)	1.9±0.6	1.8±1.0	2.5±0.8	2.7±0.8

***: $p < 0.05$**

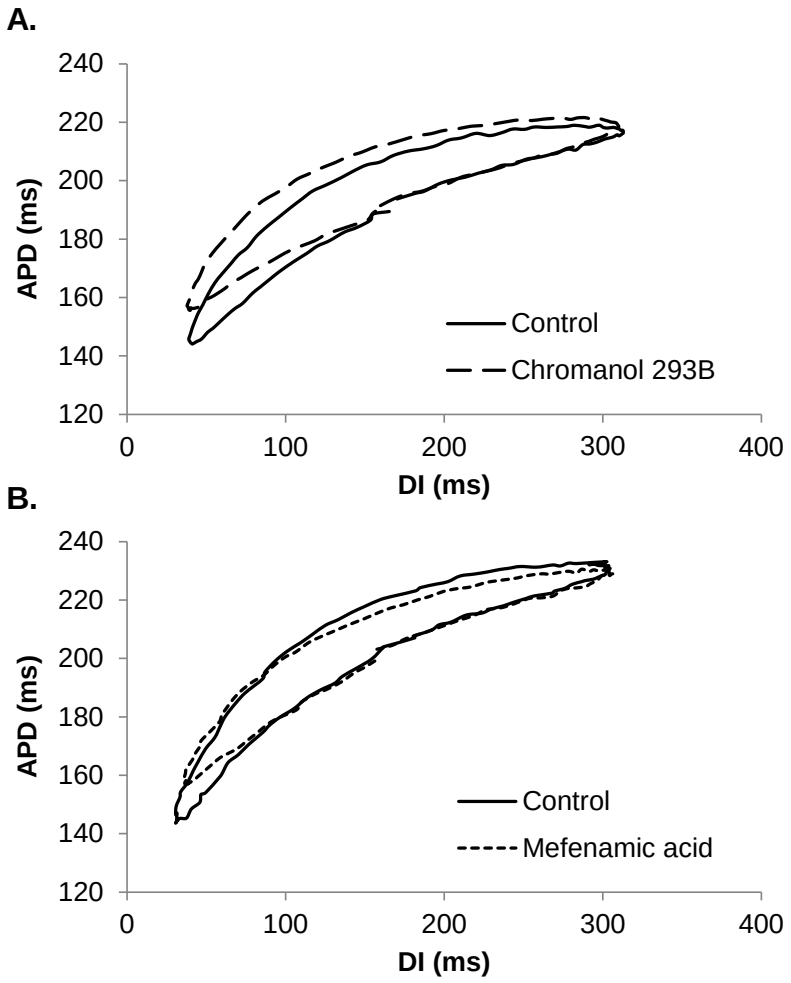

Figure 4.17 Averaged restitution relationship (N=6) of APD vs. DI during sinusoidal DI protocol with mean DI = 150 msec (protocol 3.2) for control and post-drug data.

Similar to 400 msec DI protocol, loop thickness and overall tilt were significantly different for both drugs (increase with Chromanol 293B and decrease with Mefenamic acid). As in **Figure 4.16**, the curves were vertically shifted to facilitate comparison between the hysteresis loops. Labels of the vertical axis represent APD values for the control curve.

4.9 Effects of I_{Ks} Change on APD Alternans

Alternans were induced by constant CL/DI protocols (protocol 4.1-2). For reduction of I_{Ks}, alternans occurred only in 2 animals during control, with an average amplitude of 8 msec, and alternans was observed after Chromanol 293B in 2 animals with an amplitude of 5 msec. The average CL when alternans started to occur was longer after Chromanol 293B compared with control (200 msec vs.130 msec). In all trials, activation blocked at longer CL after Chromanol 293B, i.e. average 118 msec vs. 150 msec ($p< 0.05$).

For enhancement of I_{Ks} study, alternans was present in 4 animals, all during control, with an average amplitude of 12 msec. No alternans was seen after Mefenamic acid. This result is consistent with what would be predicted by changes in the average slope of dynamic restitution, i.e. 1.19 in control vs 0.81 post-drug. The average CLs where activation block occurred were 115 msec and 106 msec for control and post-drug, respectively, with no significant difference between the two.

Figure 4.18 shows a Poincare map to represent the presence of APD alternans during control and after Mefenamic acid at CL of 180 msec in one animal. As shown in the figure, alternans was present during control and the successive APDs were divided into two clusters, while after Mefenamic acid, the alternans was suppressed and all APDs fell into one big cluster.

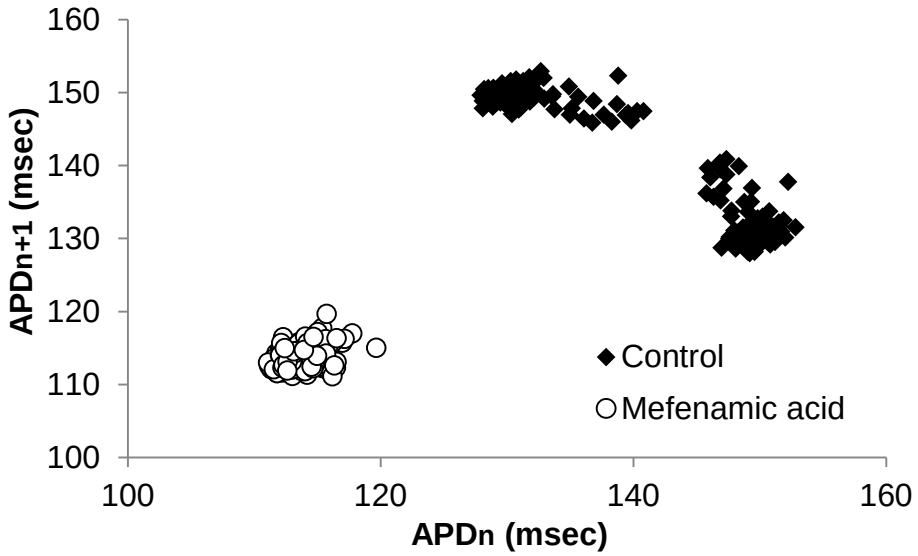

Figure 4.18 Poincare map of APD alternans during control (closed diamonds) and after Mefenamic acid (open circles).

The figure shows relationship between APD_n and APD_{n+1} at CL of 180 msec during control and after Mefenamic acid. As shown in the figure, alternans was present during control where successive APDs were separated into 2 clusters (black diamonds), while after Mefenamic acid, it was suppressed and all APDs formed one big cluster with no separations between successive APDs.

Chapter V Discussion

5.1 Hysteresis in Threshold of APD Alternans

In this phase, i.e. phase 1 of the study, the restitution-dependent mechanism of alternans was eliminated by explicitly controlling the DI using a feedback-based protocol, and hysteresis in the transition from 1:1 to 2:2 (alternans) and back to 1:1 rhythms was still observed. These results suggest that the mechanism underlying this hysteresis is distinct from the DI dependent restitution of APD and may be related to cardiac memory (hypothesis 1).

Previous studies [5, 6] have reported hysteresis in the transition between 1:1 and 2:2 rhythms. A possible explanation for the hysteresis that is observed during constant CL pacing can be visualized based on the restitution hypothesis as follows: The increase in activation rate towards shorter CLs initiates alternans by some, as yet unknown, mechanism that is dependent only on rate of activation. Once alternans are initiated, since the CL is constant, alternans of APD are always accompanied with alternans of DI with equal amplitude of alternation. Therefore, when the activation rate then decreases back to below the onset rate of alternans, APD may not stop alternating as the APD would still be affected by the alternation in preceding DI, i.e. by the restitution mechanism. As activation rate decreases further, the slope of restitution relationship becomes shallower, eventually diminishing the amplitude of alternation of DI as well as APD, resulting in a steady state, i.e. 1:1 rhythm.

However, in this phase of the study, the DIs were explicitly controlled at a constant value at each step, therefore the contribution of DI dependent restitution mechanism to alternans was eliminated. Therefore, our results indicate that there must exist mechanisms other than restitution that results in the hysteresis. Walker et al. [24] observed hysteresis in both, threshold of alternans of APD and calcium currents, suggesting that cardiac memory, i.e. the dependence of APD on the electrical history in the past several seconds, as an intrinsic property of cardiac myocytes and an important mechanism contributing to the hysteresis effect. At the same DI (or same CL in their case), we also observed larger APD alternans when DI was increasing than that when DI was decreasing (**Figure 4.4**) consistent with their findings. However, as stated before, a critical difference between study phase 1 and those reported previously is noteworthy: in this phase of the study a novel pacing protocol was used to eliminate beat by beat alterations in DIs preceding each activation, thus allowing one to explore hysteresis in the absence of restitution effects. In the previous studies, because CLs were constant, alternans of APD was always preceded by alternating DIs, therefore, the restitution effects were also always present. Results from our previous studies [21, 86] where we used sinusoidally oscillating DIs also showed that at the same DI, the average APD was smaller when DI was increasing than that when DI was decreasing. These observations suggests an interesting possibility; because at the same DI, CL was longer when DI was decreasing, if a rate of activation threshold is a mechanism of initiation of alternans, then the alternans would be expected to terminate at longer DI than the onset threshold of DI, which is consistent with the results observed in this phase of the study. However, according to this hypothesized mechanism by itself, the CL at the termination of alternans should be the same as the CL at the onset of alternans, which is

not consistent with the results of the current study (**Table 4.1**). Therefore some other mechanism(s) must come into play for the termination of alternans at longer CLs. Compared to the 30 beats stepwise DI protocol, the difference between the DIs at the onset and termination of alternans and the loop area were smaller (16 msec vs 20 msec, and 160 $msec^2$ vs 197 $msec^2$) in the 15 beats stepwise DI protocol. If cardiac memory were to affect hysteresis in alternans, as hypothesized previously, a possible explanation could be that in the 15 beats DI protocol, memory is less accumulated, at every level of DI, compared to the 30 beats DI protocol. Thus, even though APD alternans persisted after the CL reached the rate threshold, it would diminish faster as a result of less accumulated memory. The smaller difference between the amplitude of alternans during descending and ascending phases of DI could also be a result of the same phenomenon. The exact role of memory in the above scenario, however, is speculative and needs further exploration. The APD accommodation, due to increased pacing rate as seen in **Figure 4.1B** is also a possible factor contributing to the hysteresis, but if so, the mechanism is unclear. Nevertheless, the hysteresis phenomenon is the reason why once alternans is initiated, it persists even when activation rates increase and decrease around an operating mean value, a fluctuation that is often observed clinically.

In conclusion, the results of the phase 1 of the study show that even during DI-independent activation, hysteresis in thresholds for alternans onset and termination rate exists. Because the use of novel pacing protocol eliminated the effects of restitution mechanism, the observed hysteresis effect in state transition suggests that this hysteresis exists in mechanisms other than restitution.

5.2 Heterogeneous Memory in Restitution

The objective in this phase, i.e. phase 2 of the study was to determine heterogeneity in expression of memory, as quantified by hysteresis in restitution of APD, within endocardium versus epicardium and left versus right ventricles in pigs. There are two main observations of this phase of the current study: within the same ventricle, pronounced differences in parameters of memory exist between endocardium and epicardium; while between ventricles, the differences in these parameters either do not exist or are likely to be smaller than those between the endocardium and the epicardium (hypothesis 2).

In a number of previous studies [20, 26, 27, 29, 30, 32], heterogeneity in restitution of APD (not in memory) has been reported in different species, however, sometimes these results have been conflicting. For example, Pruvot et al. [33] showed that longer APD and steeper restitution were observed toward the base of right ventricle in Guinea pigs, while Nash et al. [31] and Yue et al. [92] observed that the slope of restitution was greater in the left compared to the right ventricle in humans. We observed that the restitution slopes and overall tilts (which are analogous to restitution slopes) were highest in the right ventricular endocardium in the pig. While heterogeneity in measures of memory is not very widely investigated, memory has been reported to be heterogeneous on the epicardial surface in rabbit hearts [32, 34]. Pastore et al. [93] observed, in Guinea pigs, that during alternans of APD, the standard restitution curve obtained following short APD was above the one obtained following long APD. It is interesting to note that this divergence in restitution, at the same DI, showed that when preceding DIs were decreasing, the APD was longer than the APD when the preceding DIs were increasing,

which is consistent with the hysteresis effect observed in this phase of the study. They also observed that the divergence in restitution was spatially heterogeneous on the epicardium with larger divergence near the base compared with the apex, which also suggests heterogeneous expression of memory. Results of this phase of the study suggest that in the pig, memory is expressed highest in the endocardium compared to the epicardium and the right ventricle seems to have larger memory than the left ventricle although the differences between the ventricles were not significant except for min delay, i.e. difference, in number of beats, between nadirs of APDs and DIs during sinusoidal DI protocols. Previous studies by others [18, 19, 33] and by us [15] hypothesize that memory may have dampening effect on electrical disturbances and thus increase stability. If that is the case, then results of this study suggest that in the pig, endocardial side of the heart, especially right ventricle, would be expected to be more stable and less prone to have alternans and less likely to be the site of initiation of ventricular arrhythmias. However, stability predicted using slopes of restitution leads to an opposite conclusion; endocardium in the rabbit and pig has steeper restitution curve [22, 33], thus should be a preferential site for initiation of APD alternans and of arrhythmia. Consistent with this prediction based on restitution, Laurita et al. [94] observed that calcium transient alternans occurred closer to endocardial side. Although some experimental results have been observed in agreement with the predictions based on heterogeneity in restitution, there are others which provide contrasting observations that show that arrhythmias do not always initiate from the site with steepest slope of restitution [22, 33]. Pruvot et al. reported that alternans onset occurred at the base of the left ventricle and not the right ventricle, while they observed steepest slope of the restitution in the right ventricle, a

finding inconsistent with what would be predicted by slopes of restitution. Although the species are different between their study and the phase 2 study, it is possible that the partially offsetting effects of memory on stability (more memory predicts more stability) may explain these discrepant observations because more memory may compensate the decrease in stability produced by increased slope. Once the stability has been lost and an arrhythmia such as VF is initiated, it has been suggested that, then, restitution and memory contributes only about 40% to the prediction of an APD because the correlation coefficient of a linear regression used to predict an APD during VF based on 3 previous APDs and 4 previous DIs was low [95]. However, iteration of a disturbance when memory is present becomes a non-linear process because of the distinct trajectories of restitution [15, 21]. We consider that this non-linearity may have contributed to the lower correlation coefficient that was observed when a linear regression was used to predict an APD.

The ionic basis for the differences in memory that we observed is not clear, however, it is likely to be a consequence of spatial heterogeneity in calcium handling [94]. As discussed in the background (section 2.4), intracellular calcium cycling is the hypothesized mechanism for hysteresis in restitution. Therefore, it is possible that the heterogeneous expression in calcium channels leads to the regional differences in memory. Unfortunately, although heterogeneity in Ca_i has been reported previously in dogs [94], it is not widely known whether such heterogeneity exists in the pig, making it difficult to speculate about exact ionic mechanisms behind the heterogeneity in memory in this species.

In summary, phase 2 of the current study showed that memory in restitution of APD is heterogeneously expressed in the ventricles of the pigs. We and others have predicted that memory should have a stabilizing effect on electrical disturbances. Further, the pig has been used as a model to investigate restitution and stability [18]. Therefore, these results provide an additional piece of the puzzle regarding the role of DI dependent changes in APDs, in terms of previously unknown heterogeneous expression of memory, in electrical stability in a species that has been widely used to investigate related phenomenon.

5.3 Effects of Changes in I_{Ks} on Dynamics of Repolarization

The focus of this phase, i.e. phase 3 of the study was to characterize the effects of changes in I_{Ks} on restitution and memory in swine ventricular tissue. The main observations are: 1) Chromanol 293B induced reduction of I_{Ks} in swine ventricles results in APD prolongation, and increased measures of hysteresis, i.e. memory, in restitution, but also produced steeper restitution curves. Alternans of APD was present in limited samples during both control and post-drug but occurred at longer CL post-drug; 2) enhancement of I_{Ks}, which was achieved by Mefenamic acid, shortened APD and decreased memory as well as restitution slopes, and minimized occurrence of APD alternans (hypothesis 3).

Drugs that block I_{Kr} are most common class III antiarrhythmic drugs used to prolong repolarization and prevent re-entrant arrhythmia, however, due to their reverse frequency response, that is, the dominant effect is at low heart rate or long CL while they have minimal effect at higher pacing frequency, they have limited therapeutic effect on

arrhythmia suppression and moreover, have increased risk of Torsades de Pointes [96, 97]. In the current study, results show that I_{Ks} reduction produced frequency independent changes in APDs during fast CL pacing (**Figure 4.14**). Provided that prolonging repolarization could prevent re-entrant arrhythmia and VF as shown by previous studies [43, 44], these results suggest that unlike I_{Kr}, blockade of I_{Ks} could provide potential antiarrhythmic benefit. The frequency independent effect on APD is consistent with previous studies in guinea pigs and human isolated myocytes [98], where block of I_{Ks} also produced APD prolongation at all frequencies. In contrast, studies in rabbits and canines [39, 41, 99, 100] showed minimal effects on APD after I_{Ks} blockade. Heterogeneity in I_{Ks} expression in different species and in its kinetic properties is widely reported. Presence of I_{Ks} channels in pigs and its sensitivity to Chromanol 293B has also been shown in previous studies [101, 102]. It has been reported that the kinetics of I_{Ks} in human ventricles is most similar to rabbits and dogs, but different from guinea pigs [103]. Considering the consistent observations of frequency independent changes of APDs in our study with those reported in humans, one would predict similar changes in restitution properties with manipulation of I_{Ks} in human ventricles to those observed in pigs in this phase of the study.

As discussed in chapter II, restitution of APD has been believed to be the dominant mechanism underlying initiation of APD alternans, which is conducive to re-entrant and ventricular arrhythmias [9, 12, 13, 68]. The restitution hypothesis states that, increase in slope of restitution curve indicates pro-arrhythmic effect and electrical instability. In our results, we observed an increase in restitution slope after Chromanol 293B, i.e. decrease of I_{Ks}, and a decrease in slope after Mefenamic acid, i.e. increase of I_{Ks} (**Figure 4.15**,

Table 4.5). These observations are consistent with results from our previous simulation study using the Luo-Rudy dynamic model, which is a model used to simulate action potentials of guinea pig ventricular myocyte [16]. Therefore, based on the restitution theory, our results would suggest that electrical stability in tissues with decreased I_{Ks} is compromised and it would be more susceptible to arrhythmia induction, while enhancement of I_{Ks} could stabilize electrical activation and provide antiarrhythmic protection. The results of APD alternans in this phase of the current study are partly consistent with this conclusion, where alternans was only present when the dynamic curves were steeper than 1, i.e. during both controls and after Chromanol 293B but was not present after Mefenamic acid. However, one should also note that not all situations of slope > 1 were associated with alternans. Studies [18, 19, 104, 105] related to cardiac memory have shown that restitution alone is not adequate to predict initiation of cardiac arrhythmias, rather, memory should be taken into account along with restitution to provide a more comprehensive prediction. The fact that although the slopes were consistently > 1 for all Chromanol 293B trials, alternans was only observed in 2 out of 6 animals supports this conclusion. Moreover, it is proposed that increased memory is indicative of increase in electrical stability [19, 106]. In this phase of the current study, 2 out of 5 measures of hysteresis, i.e. loop thickness and area were significantly larger (smaller) after Chromanol 293B (Mefenamic acid) (**Table 4.6** and **Table 4.7**), which suggests an increase (decrease) in memory. Therefore, in the context of the hypothesized effects of memory, our results suggest that reduction of I_{Ks} would decrease electrical stability while enhancement of I_{Ks} would have a stabilizing effect. This conclusion is opposite to that indicated by the results of restitution slopes. Therefore, the effect of I_{Ks}

manipulation, i.e. reduction and enhancement, using the contemporary hypothesized mechanisms affecting stability of activation is mixed. With presence of two offsetting components that affect stability, the ultimate effect of I_{Ks} manipulation on stability would depend on which of the two mechanisms plays a dominant role in generation of certain type of arrhythmias. Unfortunately, at this stage, without further investigations and experimental or clinical evidence, it is not clear which of the two, i.e. restitution or memory, is the predominant contributor.

The divergent effects on restitution and memory are consistent with divergent effects of changes in I_{Ks} on electrical stability that have been reported previously. For example, the increase in measures of hysteresis, i.e. in memory, provides a potential mechanism for the antiarrhythmic effect of prolonged APD during fast pacing rate through I_{Ks} blockade, as increase in memory, presumably, has a stabilizing effect on electrical activation and thus, decrease the risk of life threatening arrhythmia. A previous study [107] has shown that I_{Ks} blockade reduced dispersion of repolarization, which is a critical mechanism underlying discordant alternans and VF. However, some studies reported that suppression of I_{Ks} decreased the repolarization reserve and increased the risk of Torsades de Pointes generation [108, 109]. This phenomenon could be explained by the increased restitution slope after block of I_{Ks}. Increase in slopes of restitution decreases the electrical stability and especially when slope > 1, the probability is increased substantially for onset of APD alternans, which could lead to ventricular arrhythmias. Observations in this phase of the current study also suggest, albeit weakly, that reduction of I_{Ks} could lead to alternans at longer CL and conduction block, a prerequisite for reentry.

The agonist, L364, 373 has been reported to activate I_{Ks} in guinea pigs [90] and rabbits [91] at concentrations of 0.1 and 1 μM, but to have minimal effect in dogs [45]. Magyar et al. [45] (their figure 2) showed that at concentrations of 0.1, 1 and 3 μM, L364, 373 failed to increase I_{Ks}, except it slightly increased the time constant for deactivation of the I_{Ks} channel at the highest concentration. Observation in phase 3 of the study in using the highest concentration of this agonist as they did (3 μM) is consistent with that in dogs and suggests that, in the swine, this compound probably is not effective in enhancing I_{Ks}. Mefenamic acid is known as a blocker of Cl^- current, however, it has also been shown to increase I_{Ks} in several studies (which is also shown by Magyar et al in their figure 1) [45, 110, 111]. So, although we interpret results after Mefenamic acid as indicative of increased I_{Ks}, which is appropriate based on these previous studies, this compound may have other, non-specific, effects as well.

Results show that increase in I_{Ks} decreases slope of restitution and measures of memory (**Figure 4.15** and **Figure 4.16**), suggesting the existence of both stabilizing and destabilizing effects. Further, the results of APD alternans suggest that this drug might have a suppressive effect on alternans generation. Therapeutic usefulness of enhancement of I_{Ks} is uncertain, but it is hypothesized to be able to prevent excessive APD prolongation by increasing the repolarization reserve, which could compensate the adverse effect caused by application of I_{Kr} blocking drugs [97, 109, 112]. Nevertheless, the results on enhancement of I_{Ks} suggest that the effect of I_{Ks} activator on restitution and memory should be taken into account when considering its therapeutic benefit.

Chapter VI Conclusions

The heart is a complicated system and arrhythmias can be initiated through multiple pathways. Antiarrhythmic treatment that tries to suppress one mechanism might trigger another. Therefore, it is important to reveal all possible mechanisms and eliminate as many risk factors as possible during development of new therapies. Repolarization alternans is the cellular mechanism that causes T-wave alternans and is thought to be a precursor to ventricular arrhythmia. Majority of investigations of mechanisms of APD alternans focus on the restitution theory, although limited success has been gained in terms of arrhythmia prediction, prevention and suppression. In our previous studies, we have shown that APD alternans can occur independent of restitution, and that hysteresis, i.e. memory exists in restitution. Memory is hypothesized to have a stabilizing effect on electrical activation, and thus can offset the adverse effect of steep restitution on electrical activation. Therefore, in the current study, we focused on exploring the characteristics of hysteresis under different physiological conditions. Main observations of the current study are: 1) during DI independent pacing, hysteresis in alternans onset threshold still existed, i.e. alternans that occurred at short DI persisted even though DI increased to longer value than where alternans was initiated; 2) significant differences exist in expression of memory in different regions of the heart, with more memory in endocardium compared to epicardium; 3) enhancement (attenuation) of I_{Ks} lead to decrease in (increase) memory but meanwhile decrease (increase) in restitution slope, suggesting both stabilizing and destabilizing effect on electrical activation.

In detail, the current study suggests:

First, hysteresis in alternans threshold is not merely caused by restitution, and other unknown mechanisms are also involved (study phase 1, hypothesis 1). Clinically, it has been reported in patients that T-wave alternans, once started at higher heart rate, persist even the heart rate drops below the heart rate where the alternans was initiated. If restitution was the only responsible mechanism, then drugs that flattened restitution curves could be used for treatment. However, in previous studies [23-25], restitution cannot be separated as constant CL pacing was used. **Figure 6.1** shows an example that once alternans initiates at short CL, an increase in CL may or may not induce hysteresis depending on whether CL is increased after the long or short beat. Therefore, restitution is always involved in the constant CL pacing. In phase 1 of the study, we used a novel protocol to control DI during real time and thus eliminated the restitution mechanism, however, hysteresis in alternans threshold was still observed, suggesting that other mechanisms also play a role in the hysteresis. Therefore, in terms of clinical implication, it is not enough to just reduce the slope of restitution in order to eliminate the hysteresis and prevent arrhythmia if it is caused by alternans.

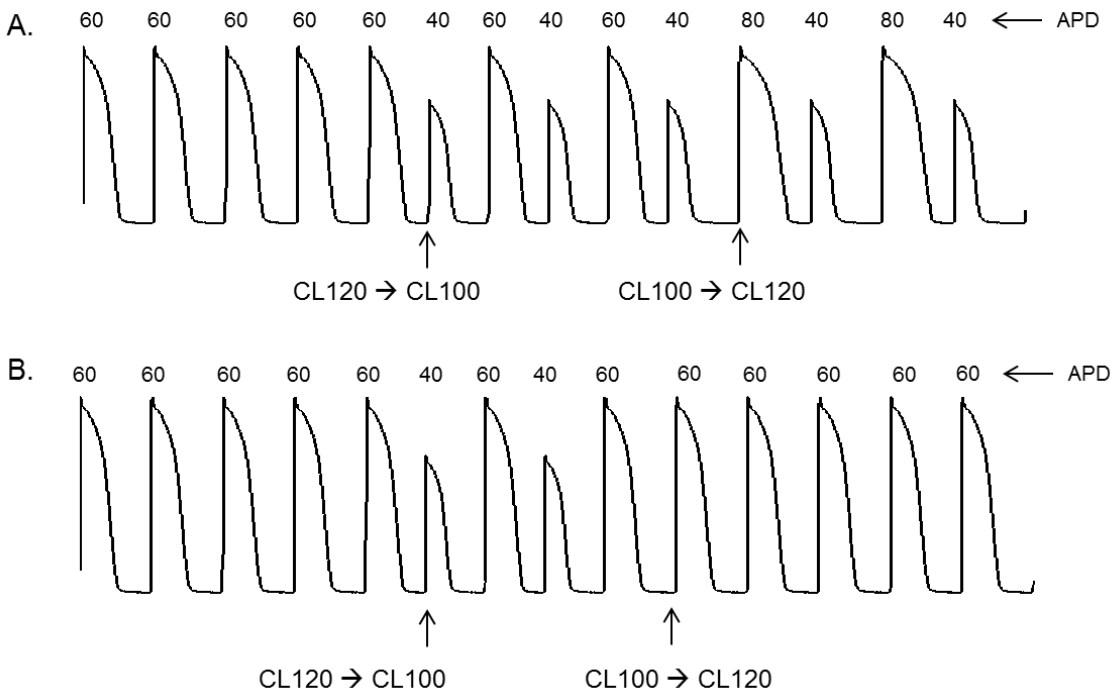

Figure 6.1 Simulated APDs to illustrate restitution induced hysteresis in alternans.

The system was at normal rhythm at CL of 120 msec and alternans is not initiated until CL reduced from 120 msec to 100 msec. The alternans amplitude is 20 msec (60 msec vs 40 msec). And then, when CL increases back to 120 msec, depending on which beat (long or short) the CL is changed, hysteresis in alternans may (A) or may not (B) occur. In panel A, CL increases to 120 msec after the short beat (APD = 40 msec), and the alternans persists to CL of 120 msec with a bigger amplitude, i.e. 20 msec alternans is magnified to 40 msec alternans. However, in panel B, CL increases to 120 msec after the long beat, and alternans is eliminated, i.e. APDs are all equal to 60 msec. The evolution of APDs is solely determined by the different DIs preceding the long and short APD, i.e. restitution.

Second, expression in hysteresis, i.e. memory is distributed differently in different types of myocytes in the heart, suggesting that the preferential location of arrhythmia initiation may be different from that predicted by restitution (study phase 2, hypothesis 2). Electrophysiological heterogeneity is an intrinsic property of the heart. Disturbance to the normal heart rhythm can be provided by a triggering event, such as nervous regulation [113], ischemia [114], and stress [115]. Development of arrhythmia through these disturbances can be facilitated by regional differences in electrical properties of the heart such as action potential morphologies, conduction velocities and dynamics of repolarization properties. During diseased conditions, electrophysiological properties may be altered in one area of the heart and result in extreme heterogeneities in APDs, restitution and memory property. These extreme heterogeneities in the heart could further lead to ventricular arrhythmia and promote spiral wave breakup. Given the importance of heterogeneity in conduction of activation, heterogeneity in restitution has been reported in previous studies, and predictions of where arrhythmia would most likely occur have been made based on the steepness of restitution. However, these predictions are often inconsistent with experimental observations. We observed, in phase 2 of the study, the heterogeneous expression of memory that was previously unknown. These results provide a reasonable explanation for these inconsistent results. As locations that have the steepest restitution slope in the heart may also have the highest memory, the ultimate stability in one area of the heart is determined by the interaction of the two, i.e. restitution and memory. Also, since memory is hypothesized to have a stabilizing effect, augmenting memory or hysteresis effect may be considered as a potential strategy to increase stability and prevent arrhythmia.

Third, drugs that enhance (minimize) I_{Ks} can decrease (increase) both restitution slope and memory, suggesting that these drugs have both beneficial and harmful effect on electrical stability (study phase 3, hypothesis 3). I_{Kr} and I_{Ks} related drugs (Class III antiarrhythmic drugs) are extensively used to treat atrial arrhythmias [116]. However, it has been reported that drugs that suppress atrial fibrillation induce life-threatening ventricular arrhythmias later on [117]. Therefore, it becomes a pressing issue to understand the possible side effect on ventricles of the antiarrhythmic drugs that are used to treat atrial arrhythmias. Although characteristics of I_{Kr} have been widely investigated, and I_{Kr} drugs often associate with torsades de pointes, little is known about I_{Ks} and its effect on electrical properties in ventricles. In this phase of the study we provided the extra piece of information about how changes in I_{Ks} could affect ventricular electrical properties. The observed results show both beneficial and harmful effect on stability for both antagonist and agonist of I_{Ks}. As increase of memory has been hypothesized to increase stability, while steeper restitution has been shown to decrease stability, the ultimate effects of these drugs depend on which mechanism (restitution or memory) plays the dominant role. Results from the phase 3 of the current study suggest that it is possible that application of I_{Ks} drugs for treatment of atrial fibrillation could have proarrhythmic risk on ventricles.

In summary, characteristics of hysteresis can vary depending on different physiological and pathological conditions, and thus, need to be taken account when predicting occurrence of arrhythmias and developing antiarrhythmic therapies.

Chapter VII Limitations

In the heterogeneity study, although we did not observe any statistically significant differences in most measures of memory in the same myocardial layers between the left and the right ventricles, it is possible that conducting the study on a larger number of animals may have revealed a difference. However, our results do suggest that even if statistically significant difference in these measures exists between the two ventricles, the differences are likely to be smaller in magnitude than the significant differences that we observed between the endocardial and the epicardial tissues.

As also reported by others in canines, we found that the equilibration time for the epicardial tissues was longer than that for the endocardial tissues, leaving open the possibility that difference in time may have contributed to the observed heterogeneity. Based on the morphologies of recorded action potentials, we consider that these effects, if any, would have been minimal. Nevertheless, the technical difficulties associated with equilibration times, tissue viability, and importantly, the requirement to have stable intracellular potential recordings that could be used in a real-time feedback loop for pacing were the reasons why we did not explore base to apex heterogeneity in addition to the endocardial to epicardial heterogeneity in this study.

In the I_{Ks} study, we used a non-selective I_{Ks} agonist to test the effect of increase in I_{Ks}. As shown in previous studies [45, 110, 111], Mefenamic acid could also inhibit Cl^- current, however, as reported before, block of Cl^- could prolong APD, so the shortening of APD observed in this study after Mefenamic acid suggests that the drug likely did activate I_{Ks} as intended. Although L364, 373 has been reported to selectively activate I_{Ks} in rodents

and rabbits, our results show it did not have an effect on APD at 500 msec CL in pigs. All of our recordings were made from endocardial side of the right ventricle. Whether similar results will be obtained from other cell types in other areas of the heart is unknown. Considering the heterogeneity of I_{Ks} expression in the heart, it is likely that changes in this current may alter electrical substrate heterogeneously as well.

Studies have shown that I_{Ks} didn't affect APD during normal conditions and a physiological impact was only observed in combination with the presence of β-adrenergic stimulation, for example, with application of isoproterenol. The current study was conducted without any β-adrenergic stimulation, therefore, it is unclear whether sympathetic stimulation plays a role in the effect of I_{Ks} changes on dynamics of repolarization.

Future studies could be focused on the following aspects. 1) The current study demonstrated that restitution is not the only mechanism involved in hysteresis in threshold of alternans, although other underlying mechanism(s) were not identified. Future study needs to determine other responsible mechanism(s) for this type of hysteresis, for example, cardiac memory. One way to accomplish this is to manipulate cardiac memory calcium current in experiments using calcium blockers or in simulation, and explore the changes of hysteresis in alternans threshold. 2) Base to apex differences in hysteresis in restitution needs to be determined in future studies, which was not included in the current study. Optical imaging studies could potentially help investigate the arrhythmia initiation location, and validate our theory about cardiac memory affecting the preferred location of arrhythmia onset. However, optical mapping could only provide information on the epicardial surface, to investigate the effect of transmural differences in

cardiac memory on arrhythmia initiation, computational simulation needs to be conducted in three-dimensional ventricular models. 3) Dosage of the I_{Ks} drugs in the current study was chosen according to previous studies. Considering the inter-species differences, effect of different doses on I_{Ks} current and on restitution and memory needs to be tested in future study. Also, regional differences in effect of I_{Ks} changes on restitution and memory can be explored using different types of myocytes in future study.

References

1. Zipes, D.P. and H.J. Wellens, *Sudden cardiac death.* Circulation, 1998. **98**(21): p. 2334-51.

2. Association, A.H., *About Cardiac Arrest.* 2013.

3. FoxNews, *Fast Facts on Cardiac Arrest From the American Heart Association. Read more: http://www.foxnews.com/story/0,2933,529112,00.html#ixzz2Ncr86JgS.* 2009.

4. Chinushi, M., et al., *Electrophysiological basis of arrhythmogenicity of QT/T alternans in the long-QT syndrome: tridimensional analysis of the kinetics of cardiac repolarization.* Circ Res, 1998. **83**(6): p. 614-28.

5. Makikallio, T.H., et al., *Abnormalities in beat to beat complexity of heart rate dynamics in patients with a previous myocardial infarction.* J Am Coll Cardiol, 1996. **28**(4): p. 1005-11.

6. Pastore, J.M., et al., *Mechanism linking T-wave alternans to the genesis of cardiac fibrillation.* Circulation, 1999. **99**(10): p. 1385-94.

7. Gold, M.R., et al., *A comparison of T-wave alternans, signal averaged electrocardiography and programmed ventricular stimulation for arrhythmia risk stratification.* J Am Coll Cardiol, 2000. **36**(7): p. 2247-53.

8. Walker, M.L. and D.S. Rosenbaum, *Repolarization alternans: implications for the mechanism and prevention of sudden cardiac death.* Cardiovasc Res, 2003. **57**(3): p. 599-614.

9. Rosenbaum, D.S., et al., *Electrical alternans and vulnerability to ventricular arrhythmias.* N Engl J Med, 1994. **330**(4): p. 235-41.

10. Berger, R.D., *Repolarization alternans: toward a unifying theory of reentrant arrhythmia induction.* Circ Res, 2000. **87**(12): p. 1083-4.

11. Hohnloser, S.H., et al., *T wave alternans as a predictor of recurrent ventricular tachyarrhythmias in ICD recipients: prospective comparison with conventional risk markers.* J Cardiovasc Electrophysiol, 1998. **9**(12): p. 1258-68.

12. Koller, M.L., M.L. Riccio, and R.F. Gilmour, Jr., *Dynamic restitution of action potential duration during electrical alternans and ventricular fibrillation.* Am J Physiol, 1998. **275**(5 Pt 2): p. H1635-42.

13. Qu, Z.L., et al., *Mechanisms of discordant alternans and induction of reentry in simulated cardiac tissue.* Circulation, 2000. **102**(14): p. 1664-1670.

14. Gilmour, R.F., Jr., N.F. Otani, and M.A. Watanabe, *Memory and complex dynamics in cardiac Purkinje fibers.* Am J Physiol, 1997. **272**(4 Pt 2): p. H1826-32.

15. Wu, R. and A. Patwardhan, *Restitution of action potential duration during sequential changes in diastolic intervals shows multimodal behavior.* Circ Res, 2004. **94**(5): p. 634-41.

16. Wu, R. and A. Patwardhan, *Effects of rapid and slow potassium repolarization currents and calcium dynamics on hysteresis in restitution of action potential duration.* J Electrocardiol, 2007. **40**(2): p. 188-99.

17. Wu, R. and A. Patwardhan, *Mechanism of repolarization alternans has restitution of action potential duration dependent and independent components.* J Cardiovasc Electrophysiol, 2006. **17**(1): p. 87-93.

18. Banville, I., N. Chattipakorn, and R.A. Gray, *Restitution dynamics during pacing and arrhythmias in isolated pig hearts.* J Cardiovasc Electrophysiol, 2004. **15**(4): p. 455-63.

19. Cherry, E.M. and F.H. Fenton, *Suppression of alternans and conduction blocks despite steep APD restitution: electrotonic, memory, and conduction velocity restitution effects.* Am J Physiol Heart Circ Physiol, 2004. **286**(6): p. H2332-41.

20. Selvaraj, R.J., et al., *Steeper restitution slopes across right ventricular endocardium in patients with cardiomyopathy at high risk of ventricular arrhythmias.* Am J Physiol Heart Circ Physiol, 2007. **292**(3): p. H1262-8.

21. Guzman, K.M., L. Jing, and A. Patwardhan, *Effects of changes in the L-type calcium current on hysteresis in restitution of action potential duration.* Pacing Clin Electrophysiol, 2010. **33**(4): p. 451-9.

22. Lu, J.J., et al., *[Transmural heterogeneity of calcium handling proteins in the mechanism of porcine model of ventricular fibrillation]*. Zhonghua Xin Xue Guan Bing Za Zhi, 2008. **36**(4): p. 355-9.

23. Hall, G.M., S. Bahar, and D.J. Gauthier, *Prevalence of rate-dependent behaviors in cardiac muscle.* Physical Review Letters, 1999. **82**(14): p. 2995-2998.

24. Walker, M.L., et al., *Hysteresis effect implicates calcium cycling as a mechanism of repolarization alternans.* Circulation, 2003. **108**(21): p. 2704-9.

25. Yehia, A.R., et al., *Hysteresis and bistability in the direct transition from 1:1 to 2:1 rhythm in periodically driven single ventricular cells.* Chaos, 1999. **9**(4): p. 916-931.

26. Banville, I. and R.A. Gray, *Effect of action potential duration and conduction velocity restitution and their spatial dispersion on alternans and the stability of arrhythmias.* J Cardiovasc Electrophysiol, 2002. **13**(11): p. 1141-9.

27. Clayton, R.H. and P. Taggart, *Regional differences in APD restitution can initiate wavebreak and re-entry in cardiac tissue: a computational study.* Biomed Eng Online, 2005. **4**: p. 54.

28. Extramiana, F. and C. Antzelevitch, *Amplified transmural dispersion of repolarization as the basis for arrhythmogenesis in a canine ventricular-wedge model of short-QT syndrome.* Circulation, 2004. **110**(24): p. 3661-6.

29. Keldermann, R.H., et al., *Effect of heterogeneous APD restitution on VF organization in a model of the human ventricles.* Am J Physiol Heart Circ Physiol, 2008. **294**(2): p. H764-74.

30. Taggart, P. and M. Lab, *Cardiac mechano-electric feedback and electrical restitution in humans.* Prog Biophys Mol Biol, 2008. **97**(2-3): p. 452-60.

31. Nash, M.P., et al., *Whole heart action potential duration restitution properties in cardiac patients: a combined clinical and modelling study.* Exp Physiol, 2006. **91**(2): p. 339-54.

32. Pitruzzello, A.M., W. Krassowska, and S.F. Idriss, *Spatial heterogeneity of the restitution portrait in rabbit epicardium.* Am J Physiol Heart Circ Physiol, 2007. **292**(3): p. H1568-78.

33. Pruvot, E.J., et al., *Role of calcium cycling versus restitution in the mechanism of repolarization alternans.* Circ Res, 2004. **94**(8): p. 1083-90.

34. Mironov, S., J. Jalife, and E.G. Tolkacheva, *Role of conduction velocity restitution and short-term memory in the development of action potential duration alternans in isolated rabbit hearts.* Circulation, 2008. **118**(1): p. 17-25.

35. Abi-Gerges, N., et al., *Gender differences in the slow delayed (IKs) but not in inward (IK1) rectifier K+ currents of canine Purkinje fibre cardiac action potential: key roles for IKs, beta-adrenoceptor stimulation, pacing rate and gender.* Br J Pharmacol, 2006. **147**(6): p. 653-60.

36. Roden, D.M., *Ionic mechanisms for prolongation of refractoriness and their proarrhythmic and antiarrhythmic correlates.* Am J Cardiol, 1996. **78**(4A): p. 12-6.

37. Nair, L.A. and A.O. Grant, *Emerging class III antiarrhythmic agents: mechanism of action and proarrhythmic potential.* Cardiovasc Drugs Ther, 1997. **11**(2): p. 149-67.

38. Cheng, J.H. and I. Kodama, *Two components of delayed rectifier K+ current in heart: molecular basis, functional diversity, and contribution to repolarization.* Acta Pharmacol Sin, 2004. **25**(2): p. 137-45.

39. Lengyel, C., et al., *Pharmacological block of the slow component of the outward delayed rectifier current (I(Ks)) fails to lengthen rabbit ventricular muscle QT(c) and action potential duration.* Br J Pharmacol, 2001. **132**(1): p. 101-10.

40. Lu, Z., et al., *Density and kinetics of I(Kr) and I(Ks) in guinea pig and rabbit ventricular myocytes explain different efficacy of I(Ks) blockade at high heart rate in guinea pig and rabbit: implications for arrhythmogenesis in humans.* Circulation, 2001. **104**(8): p. 951-6.

41. Stengl, M., et al., *Accumulation of slowly activating delayed rectifier potassium current (IKs) in canine ventricular myocytes.* J Physiol, 2003. **551**(Pt 3): p. 777-86.

42. Dorian, P. and D. Newman, *Rate dependence of the effect of antiarrhythmic drugs delaying cardiac repolarization: an overview.* Europace, 2000. **2**(4): p. 277-85.

43. Singh, B.N., *Control of cardiac arrhythmias by lengthening repolarization*1988, Mount Kisco, N.Y.: Futura Pub. Co. 596 p.

44. Singh, B.N. and E.M. Vaughan Williams, *A third class of anti-arrhythmic action. Effects on atrial and ventricular intracellular potentials, and other pharmacological actions on cardiac muscle, of MJ 1999 and AH 3474.* Br J Pharmacol, 1970. **39**(4): p. 675-87.

45. Magyar, J., et al., *L-364,373 fails to activate the slow delayed rectifier K+ current in canine ventricular cardiomyocytes.* Naunyn Schmiedebergs Arch Pharmacol, 2006. **373**(1): p. 85-9.

46. Samie, F.H. and J. Jalife, *Mechanisms underlying ventricular tachycardia and its transition to ventricular fibrillation in the structurally normal heart.* Cardiovasc Res, 2001. **50**(2): p. 242-50.

47. Pastore, J.M. and D.S. Rosenbaum, *Role of structural barriers in the mechanism of alternans-induced reentry.* Circ Res, 2000. **87**(12): p. 1157-63.

48. Karagueuzian, H.S. and P.S. Chen, *Cellular mechanism of reentry induced by a strong electrical stimulus: implications for fibrillation and defibrillation.* Cardiovasc Res, 2001. **50**(2): p. 251-62.

49. Gilmour, R.F., Jr. and D.R. Chialvo, *Electrical restitution, critical mass, and the riddle of fibrillation.* J Cardiovasc Electrophysiol, 1999. **10**(8): p. 1087-9.

50. Libbus, I. and D.S. Rosenbaum, *Remodeling of cardiac repolarization: mechanisms and implications of memory.* Card Electrophysiol Rev, 2002. **6**(3): p. 302-10.

51. Davidenko, J.M., et al., *Stationary and drifting spiral waves of excitation in isolated cardiac muscle.* Nature, 1992. **355**(6358): p. 349-51.

52. Gray, R.A., et al., *Nonstationary Vortex-Like Reentrant Activity as a Mechanism of Polymorphic Ventricular-Tachycardia in the Isolated Rabbit Heart.* Circulation, 1995. **91**(9): p. 2454-2469.

53. Janse, M.J., F.J.G. Wilmsschopman, and R. Coronel, *Ventricular-Fibrillation Is Not Always Due to Multiple Wavelet Reentry.* Journal of Cardiovascular Electrophysiology, 1995. **6**(7): p. 512-521.

54. Samie, F.H., et al., *Rectification of the background potassium current - A determinant of rotor dynamics in ventricular fibrillation.* Circulation Research, 2001. **89**(12): p. 1216-1223.

55. Bayly, P.V., et al., *Spatial organization, predictability, and determinism in ventricular fibrillation.* Chaos, 1998. **8**(1): p. 103-115.

56. Kim, Y.H., et al., *Mechanism of procainamide-induced prevention of spontaneous wave break during ventricular fibrillation - Insight into the maintenance of fibrillation wave fronts.* Circulation, 1999. **100**(6): p. 666-674.

57. Witkowski, F.X., et al., *Spatiotemporal evolution of ventricular fibrillation.* Nature, 1998. **392**(6671): p. 78-82.

58. Walcott, G.P., et al., *Endocardial wave front organization during ventricular fibrillation in humans.* J Am Coll Cardiol, 2002. **39**(1): p. 109-15.

59. Klabunde, R.E., *Cardiovascular Physiology Concepts.* *http://www.cvphysiology.com/Arrhythmias/A008c.htm*.

60. Sherwood, L., *Human Physiology: From Cells to Systems.*2012.

61. Zipes, D.P., J.C. Bailey, and V. Elharrar, *The Slow inward current and cardiac arrhythmias*. Developments in cardiovascular medicine1980, The Hague ; Boston

Hingham, MA: Martinus Nijhoff ; distributors for the U.S. and Canada, Kluwer Boston. xiii, 521 p.

62. Fenton, F.H., et al., *Multiple mechanisms of spiral wave breakup in a model of cardiac electrical activity.* Chaos, 2002. **12**(3): p. 852-892.

63. Kalb, S.S., et al., *The restitution portrait: A new method for investigating rate-dependent restitution.* Journal of Cardiovascular Electrophysiology, 2004. **15**(6): p. 698-709.

64. Koller, M.L., M.L. Riccio, and R.F. Gilmour, *Dynamic restitution of action potential duration during electrical alternans and ventricular fibrillation.* American Journal of Physiology-Heart and Circulatory Physiology, 1998. **44**(5): p. H1635-H1642.

65. Qu, Z., J.N. Weiss, and A. Garfinkel, *Cardiac electrical restitution properties and stability of reentrant spiral waves: a simulation study.* Am J Physiol, 1999. **276**(1 Pt 2): p. H269-83.

66. Riccio, M.L., M.L. Koller, and R.F. Gilmour, *Electrical restitution and spatiotemporal organization during ventricular fibrillation.* Circulation Research, 1999. **84**(8): p. 955-963.

67. Nolasco, J.B. and R.W. Dahlen, *A graphic method for the study of alternation in cardiac action potentials.* J Appl Physiol, 1968. **25**(2): p. 191-6.

68. Karma, A., *Electrical alternans and spiral wave breakup in cardiac tissue.* Chaos, 1994. **4**(3): p. 461-472.

69. Myles, R.C., et al., *Alternans of action potential duration and amplitude in rabbits with left ventricular dysfunction following myocardial infarction.* J Mol Cell Cardiol, 2011. **50**(3): p. 510-21.

70. Karagueuzian, H.S., et al., *Action potential alternans and irregular dynamics in quinidine-intoxicated ventricular muscle cells. Implications for ventricular proarrhythmia.* Circulation, 1993. **87**(5): p. 1661-72.

71. Garfinkel, A., et al., *Preventing ventricular fibrillation by flattening cardiac restitution.* Proceedings of the National Academy of Sciences of the United States of America, 2000. **97**(11): p. 6061-6066.

72. Fox, J.J., E. Bodenschatz, and R.F. Gilmour, Jr., *Period-doubling instability and memory in cardiac tissue.* Phys Rev Lett, 2002. **89**(13): p. 138101.

73. Chialvo, D.R., D.C. Michaels, and J. Jalife, *Supernormal Excitability as a Mechanism of Chaotic Dynamics of Activation in Cardiac Purkinje-Fibers.* Circulation Research, 1990. **66**(2): p. 525-545.

74. Elharrar, V. and B. Surawicz, *Cycle length effect on restitution of action potential duration in dog cardiac fibers.* Am J Physiol, 1983. **244**(6): p. H782-92.

75. Otani, N.F. and R.F. Gilmour, *Memory models for the electrical properties of local cardiac systems.* Journal of Theoretical Biology, 1997. **187**(3): p. 409-436.

76. Tolkacheva, E.G., et al., *Condition for alternans and stability of the 1 : 1 response pattern in a "memory" model of paced cardiac dynamics.* Physical Review E, 2003. **67**(3): p. -.

77. Walker, M.L., et al., *Hysteresis effect implicates calcium cycling as a mechanism of repolarization alternans.* Circulation, 2003. **108**(21): p. 2704-2709.

78. Guzman, K.M., L. Jing, and A. Patwardhan, *Effects of changes in the L-type calcium current on hysteresis in restitution of action potential duration.* Pacing Clin Electrophysiol. **33**(4): p. 451-9.

79. Fox, J.J., J.L. McHarg, and R.F. Gilmour, Jr., *Ionic mechanism of electrical alternans.* Am J Physiol Heart Circ Physiol, 2002. **282**(2): p. H516-30.

80. Hua, F. and R.F. Gilmour, Jr., *Contribution of IKr to rate-dependent action potential dynamics in canine endocardium.* Circ Res, 2004. **94**(6): p. 810-9.

81. Roden, D.M., *Drug-Therapy - Risks and Benefits of Antiarrhythmic Therapy.* New England Journal of Medicine, 1994. **331**(12): p. 785-791.

82. Roden, D.M., *Drug-induced prolongation of the QT interval.* N Engl J Med, 2004. **350**(10): p. 1013-22.

83. Yang, T. and D.M. Roden, *Extracellular potassium modulation of drug block of IKr. Implications for torsade de pointes and reverse use-dependence.* Circulation, 1996. **93**(3): p. 407-11.

84. Lengyel, C., et al., *Combined pharmacological block of I(Kr) and I(Ks) increases short-term QT interval variability and provokes torsades de pointes.* Br J Pharmacol, 2007. **151**(7): p. 941-51.

85. Anyukhovsky, E.P., E.A. Sosunov, and M.R. Rosen, *Regional differences in electrophysiological properties of epicardium, midmyocardium, and endocardium. In vitro and in vivo correlations.* Circulation, 1996. **94**(8): p. 1981-8.

86. Jing, L., S. Chourasia, and A. Patwardhan, *Heterogeneous memory in restitution of action potential duration in pig ventricles.* J Electrocardiol, 2010. **43**(5): p. 425-32.

87. Sun, Z.Q., G.P. Thomas, and C. Antzelevitch, *Chromanol 293B inhibits slowly activating delayed rectifier and transient outward currents in canine left ventricular myocytes.* J Cardiovasc Electrophysiol, 2001. **12**(4): p. 472-8.

88. Antzelevitch, C., et al., *Heterogeneity within the ventricular wall. Electrophysiology and pharmacology of epicardial, endocardial, and M cells.* Circ Res, 1991. **69**(6): p. 1427-49.

89. Stankovicova, T., et al., *M cells and transmural heterogeneity of action potential configuration in myocytes from the left ventricular wall of the pig heart.* Cardiovasc Res, 2000. **45**(4): p. 952-60.

90. Salata, J.J., et al., *A novel benzodiazepine that activates cardiac slow delayed rectifier K+ currents.* Molecular Pharmacology, 1998. **54**(1): p. 220-30.

91. Xu, X., et al., *Increasing I(Ks) corrects abnormal repolarization in rabbit models of acquired LQT2 and ventricular hypertrophy.* Am J Physiol Heart Circ Physiol, 2002. **283**(2): p. H664-70.

92. Yue, A.M., et al., *Global endocardial electrical restitution in human right and left ventricles determined by noncontact mapping.* J Am Coll Cardiol, 2005. **46**(6): p. 1067-75.

93. Pastore, J.M., K.R. Laurita, and D.S. Rosenbaum, *Importance of spatiotemporal heterogeneity of cellular restitution in mechanism of arrhythmogenic discordant alternans.* Heart Rhythm, 2006. **3**(6): p. 711-9.

94. Laurita, K.R., et al., *Transmural heterogeneity of calcium handling in canine.* Circ Res, 2003. **92**(6): p. 668-75.

95. Huang, J., et al., *Restitution properties during ventricular fibrillation in the in situ swine heart.* Circulation, 2004. **110**(20): p. 3161-7.

96. Nattel, S. and F.D. Zeng, *Frequency-dependent effects of antiarrhythmic drugs on action potential duration and refractoriness of canine cardiac Purkinje fibers.* J Pharmacol Exp Ther, 1984. **229**(1): p. 283-91.

97. Barhanin, J., B. Attali, and M. Lazdunski, *IKs, a slow and intriguing cardiac K+ channel and its associated long QT diseases.* Trends Cardiovasc Med, 1998. **8**(5): p. 207-14.

98. Bosch, R.F., et al., *Effects of the chromanol 293B, a selective blocker of the slow, component of the delayed rectifier K+ current, on repolarization in human and guinea pig ventricular myocytes.* Cardiovasc Res, 1998. **38**(2): p. 441-50.

99. Guerard, N.C., et al., *Selective block of IKs plays a significant role in MAP triangulation induced by IKr block in isolated rabbit heart.* J Pharmacol Toxicol Methods, 2008. **58**(1): p. 32-40.

100. Volders, P.G., et al., *Probing the contribution of IKs to canine ventricular repolarization: key role for beta-adrenergic receptor stimulation.* Circulation, 2003. **107**(21): p. 2753-60.

101. Laursen, M., et al., *Characterization of cardiac repolarization in the Gottingen minipig.* J Pharmacol Toxicol Methods, 2011. **63**(2): p. 186-95.

102. Verkerk, A.O., et al., *Incorporated sarcolemmal fish oil fatty acids shorten pig ventricular action potentials.* Cardiovasc Res, 2006. **70**(3): p. 509-20.

103. Virag, L., et al., *The slow component of the delayed rectifier potassium current in undiseased human ventricular myocytes.* Cardiovasc Res, 2001. **49**(4): p. 790-797.

104. Choi, B.R., T. Liu, and G. Salama, *Adaptation of cardiac action potential durations to stimulation history with random diastolic intervals.* J Cardiovasc Electrophysiol, 2004. **15**(10): p. 1188-97.

105. Jordan, P.N. and D.J. Christini, *Determining the effects of memory and action potential duration alternans on cardiac restitution using a constant-memory restitution protocol.* Physiol Meas, 2004. **25**(4): p. 1013-24.

106. Chialvo, D.R., D.C. Michaels, and J. Jalife, *Supernormal Excitability as a Mechanism of Chaotic Dynamics of Activation in Cardiac Purkinje-Fibers.* Circ Res, 1990. **66**(2): p. 525-545.

107. Pajouh, M., et al., *IKs blockade reduces dispersion of repolarization in heart failure.* Heart Rhythm, 2005. **2**(7): p. 731-8.

108. Cheng, H.C. and J. Incardona, *Models of torsades de pointes: effects of FPL64176, DPI201106, dofetilide, and chromanol 293B in isolated rabbit and guinea pig hearts.* J Pharmacol Toxicol Methods, 2009. **60**(2): p. 174-84.

109. Jost, N., J.G. Papp, and A. Varro, *Slow delayed rectifier potassium current (IKs) and the repolarization reserve.* Ann Noninvasive Electrocardiol, 2007. **12**(1): p. 64-78.

110. Busch, A.E., et al., *The role of the IsK protein in the specific pharmacological properties of the IKs channel complex.* Br J Pharmacol, 1997. **122**(2): p. 187-9.

111. Busch, A.E., et al., *Positive Regulation by Chloride Channel Blockers of I-Sk Channels Expressed in Xenopus Oocytes.* Molecular Pharmacology, 1994. **46**(4): p. 750-753.

112. Liu, Z., L. Du, and M. Li, *Update on the slow delayed rectifier potassium current (I(Ks)): role in modulating cardiac function.* Curr Med Chem, 2012. **19**(9): p. 1405-20.

113. De Jong, M.J. and D.C. Randall, *Heart rate variability analysis in the assessment of autonomic function in heart failure.* J Cardiovasc Nurs, 2005. **20**(3): p. 186-95; quiz 196-7.

114. Rodriguez, B., J.M. Ferrero, Jr., and B. Trenor, *Mechanistic investigation of extracellular K+ accumulation during acute myocardial ischemia: a simulation study.* Am J Physiol Heart Circ Physiol, 2002. **283**(2): p. H490-500.

115. Randall, D.C., et al., *Ablation of posterior atrial ganglionated plexus potentiates sympathetic tachycardia to behavioral stress.* Am J Physiol, 1998. **275**(3 Pt 2): p. R779-87.

116. Singh, B.N. and N. Wadhani, *Antiarrhythmic and proarrhythmic properties of QT-prolonging antianginal drugs.* J Cardiovasc Pharmacol Ther, 2004. **9 Suppl 1**: p. S85-97.

117. Kolb, C., G. Ndrepepa, and B. Zrenner, *Late dofetilide-associated life-threatening proarrhythmia.* Int J Cardiol, 2008. **127**(2): p. e54-6.

Vita

Author's Name: Linyuan Jing

Birthplace: Shandong, China

Education:

B.E. in Biomedical Engineering, Shandong University, China June 2008

Publications related to this dissertation:

1. Jing Linyuan, Patwardhan Abhijit. Hysteresis in DI Independent Mechanisms in Threshold for Transition between 1:1 and 2:2 Rhythms in Pigs. Conf Proc IEEE Eng Med Biol Soc. 2012; 2012: 665-8.
2. Jing Linyuan, Chourasia Sonam, Patwardhan Abhijit. Heterogeneous memory in restitution of action potential duration in pig ventricles. Journal of Electrocardiology. 2010 Sep-Oct; 43(5): 425-32

Other publications:

1. Jing Linyuan, Agarwal Anuj, Chourasia Sonam, Patwardhan Abhijit. Phase relationship between alternans of early and late phases of ventricular action potentials. Front. Physio. 2012, 3:190.
2. Agarwal Anuj, Jing Linyuan, Patwardhan Abhijit. Effect of Rapid Delayed Rectifier Current on Hysteresis in Restitution of Action Potential Duration in Swine. Conf Proc IEEE Eng Med Biol Soc. 2012; 2012: 673-6.
3. Guzman Kathleen, Jing Linyuan, Patwardhan Abhijit. Effects of Changes in the L-Type Calcium Current on Hysteresis in Restitution of Action Potential Duration. Pacing Clin Electrophysiol. 2009 Dec 10. PMID: 20015128